University of Stavanger

FACULTY OF SCIENCE AND TECHNOLOGY

MASTER'S THESIS

Study programme/specialisation:	Spring/ Autumn semester, 20.....
Environmental engineering- Water science and Technology	Spring 2021, Open
	Open / Confidential

Author: Mats Gjønnes Grendal

Programme coordinator: Roald Kommedal

Supervisor(s): Espen Enge

Title of master's thesis:

Anthropogenic impacts on Hunnedalen watershed; monitored and modeled water chemistry

Credits: 30

Keywords:	Number of pages: 45
Water chemistry	
Anthropogenic impact	+ supplemental material/other: 13
Acidification	
	Stavanger, 15.06.21
	date/year

Abstract

Hunnedalen watershed, in southwestern Norway, are associated with dilute water quality which makes it highly responsive to changes. In this study, the watershed's water quality was monitored for one year, 2020, to evaluate the anthropogenic effects on the watershed. Anthropogenic effects were found to be neglectable, however simulations demonstrated a marginally improved water quality when the watershed is regulated. The watershed was found to be highly dominated by marine ions, distributed geographically with the altitude. Further, the marine contribution was found to consume alkalinity and lower the pH in the watershed. This decrease in pH was found to mobilize inorganic aluminum. Further, the inorganic aluminum was found to be limited by humic acid and alkalinity.

The low alkalinity and humic acid concentration, especially in the high-altitude area, makes the watershed susceptible to acidification. Therefore, liming is a suggested counter measure to be sure that the fish population survives.

Preface

I am very grateful for the guidance from my supervisor, Espen Enge. The involvement and help with analysis and corrections have been of great importance for the quality of this thesis.

The fieldwork has been demanding and included a total of 156 samples sampled at every seasons of the year. A total of 2710 analysis were preformed manually.

For their assistance in the fieldwork, I would like to thank Mariane Brustugun, Victor Bo Larsen, William Bossum Arnli, Zoe Longenecker-Wright, and Kompis (our golden retriever). Further, I would like to thank Henrik van der Hoeven, Samuel Lutz, Ravn Løland-Gundersen, James W. F. Fanuelsen, and Markus Ottesen for their assistance in the laboratory.

Mats Gjønnes Grendal

Stavanger, June 2021

Table of Contents

Table of Figures

Table of tables

1 Introduction

Hunnedalen watershed is ranging from 0 m to 1100 m above sea level in Rogaland county in south western Norway. The watershed is characterized by high annual precipitation and slow weathering bedrock. This makes the area susceptible for acidification and the water quality is often dilute.

Fish death in southern Norway was reported from multiple sources in the late 1800's and early 1900's, the same period as the industrial revolution started (Dahl, 1921; Huitfeldt-Kaas, 1922). A total area of 4300 km^2 in Rogaland was affected by the acid rain in the late 1800's and early 1900's (Snekvik, 1974). Acid rain was concluded to be the cause of the fish death (Drabløs & Tollan, 1980), and recent calculations showcased that the sulfur concentration during this time period affected the water quality to a degree that exceeded the survivability of the fish population (Mylona, 1993; Schoepp et al., 2003).

The water quality of the watershed has recovered from the acidic rain during the 1900's and was found to be limitedly affected by acidification (Enge, 2013). Further, stocked fish populations were reported as stable in the last two decades (Enge, 2020b).

The water was also affected by anthropogenic activities. The highest altitude part of Hunnedalen watershed, including Lake Hunnevatn, was regulated in 1983, and the water from the upper part was being pumped out of the watershed to be utilized for hydro power. Further, runoff from the several farms and agricultural activities could increase the rivers concentration of nutrients such as phosphate and nitrate. The 855 cabins (*Statistisk sentralbyrå (Statistics Norway)*, n.d.) in Gjesdal municipality, along with mountain hikers could also increase the nutrient concentrations. Runoff from the county road, and construction work in relation to the road, was also a potential source of nutrients, ions, and oils.

The objective of this thesis is to evaluate the anthropogenic effects on the water chemistry in Hunnedalen watershed, and the potential effects on the fish population. This was done by monitoring of the water quality in the watershed for one year, 2020. Further, original pH and alkalinity was estimated to evaluate the state of the acidification of the watershed. Water chemistry was also modelled for an unregulated watershed.

2 Study area

The study took place in Gjesdal and Sirdal municipality, in Rogaland and Adger county respectively, southern Norway. Hunnedalen watershed, ranging from 0 m a.s.l. to 1100 m a.s.l., was studied. The watershed is a steep valley, starting in the mountains in east and ending by the ocean in west.

2.1 Geology

Southwestern Norway's bedrock is of Precambrian origin and consists primarily of gneiss and granite, which are slow weathering minerals(*Berggrunn (National Bedrock Database)*, n.d.). As a cause of the poor contribution of ions from the bedrock, waters associated with this geology often has a low buffer capacity. However, locally good water chemistry has been reported (Enge, 2005) caused by rock dumping in relation to roadwork.

2.2 Climate

An average annual precipitation of the watershed was estimated to be 2509,4 mm with a total area of 157,75 km^2 (Figure 2-1) (*NVE (Noregs Vassdrags- Og Energidirektorat)*, n.d.).

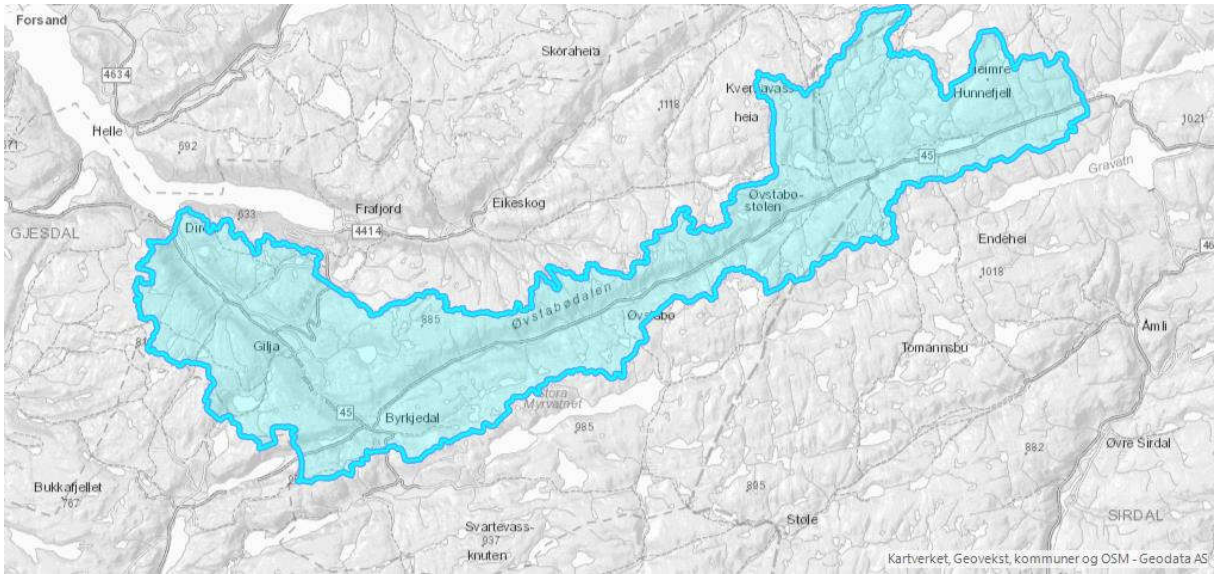

Figure 2-1 Precipitation map of Hunnedalen watershed (NVE Atles, n.d.).

Maudal and Sinnes weather stations are located 2,4 km south of Byrkjedal and 10 km east of Hunnevatn, respectively. The annual precipitation in 2020 was measured to be 4457.6 mm and 2280.5 mm, respectively (*MET (Meteorological Institute)*, n.d.). This corresponds to 142.5 % and 136.9 % of the 1990-2020 normal annual precipitation, respectively(*MET (Meteorological Institute)*, n.d.). The relatively driest and wettest months with respect to the

1990-2020 normal monthly precipitation was November 2019 and February 2020, respectively (Figure 2-2, a). The winter months are dominated with precipitation as snowfall.

Even though the spring and summer are periods of less precipitation, the runoff rates are relatively high due to snowmelt (Figure 2-2, b). The opposite effect can be seen in the main months of snowfall, November to February, where the runoff rate is relatively low compared to the precipitation.

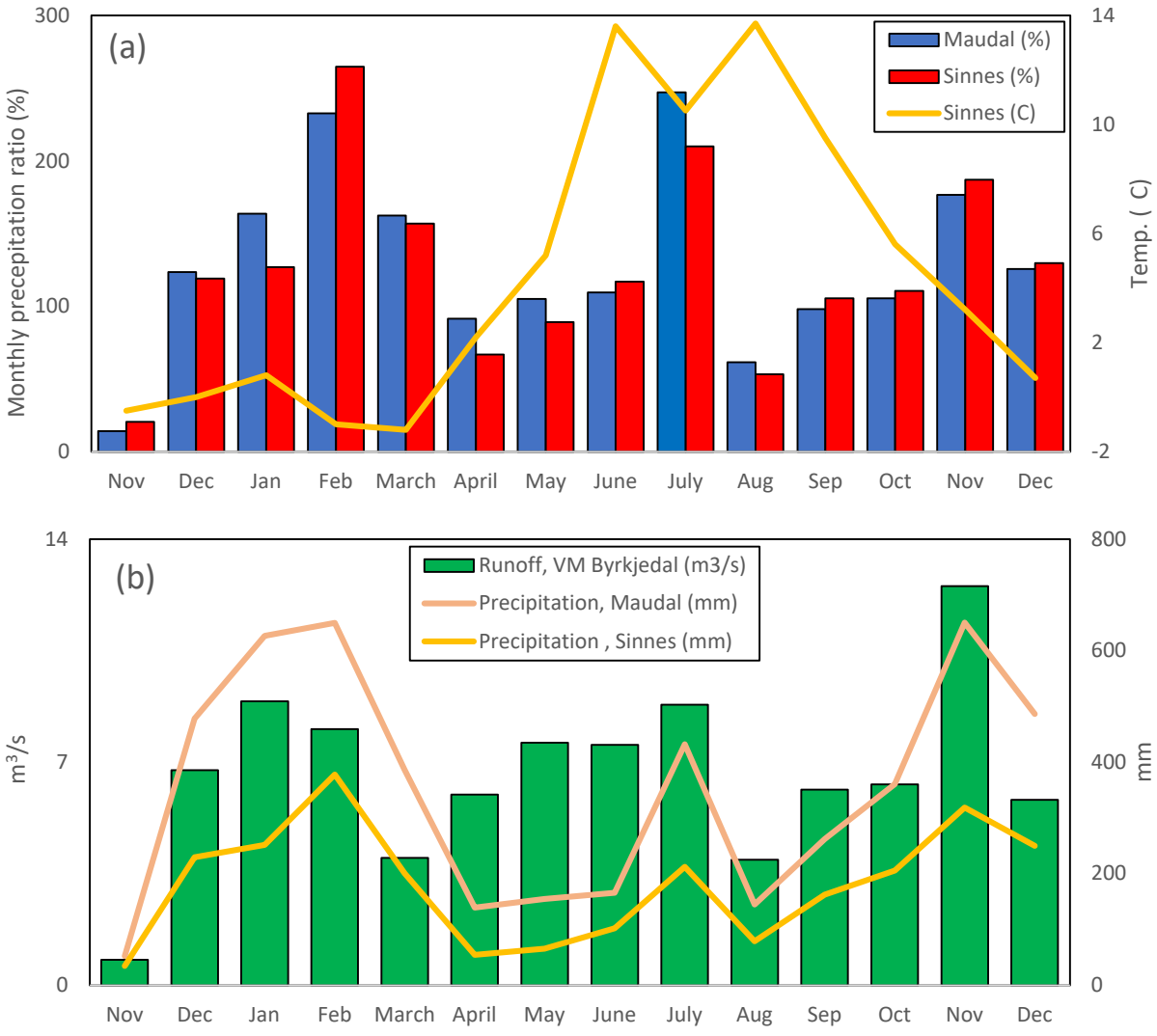

Figure 2-2 (a) Monthly precipitation ratio (%) compared to the monthly middle precipitation 1991-2020. (b) Monthly runoff (m^3/s) at VM byrkjedal limnigraph at primary axis. Secondary axis shows the monthly precepitation at Maudal and Sinnes weather station. Both figures are ranging from November 2019 to December 2020.

Data recorded at Maudal from 1947 to 2020 indicated an annual increase of precipitation with 11.7 mm ($P<0.001$) (Figure 2-3). This trend is consistent with the relatively high observed precipitation data (Figure 2-2, a).

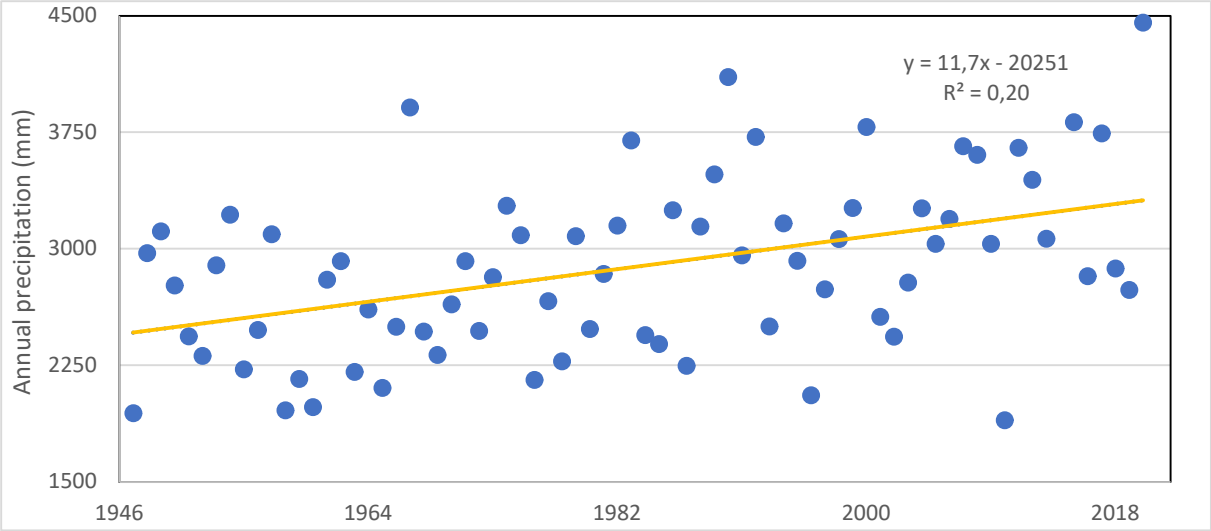

Figure 2-3 Annual precipitation (mm) at Maudal weather station from 1947 to 2020.

2.3 Historical water chemistry

Massive fish death was reported in the late 1800's and early 1900's, discussed in 2.6. This was concluded to be caused by the acid rain following the industrial revolution (Drabløs & Tollan, 1980). Calculation in later years concluded that the sulfur concentration during this time period exceeded what the fish population could withstand (Mylona, 1993; Schoepp et al., 2003). A decline or extinction of fish population was reported in 1860-1890 in multiple lakes in Rogaland and Vest-Agder (Enge, Qvenild, et al., 2017). Further, pH values for lakes in the same area ranged from 4.6-5.4, measurements conducted from 1926 to 1952 (Enge, Qvenild, et al., 2017).

It was found that the pH in Lake Djupavatn, in Hunnedalen watershed, was around 4.9 in the years 1972-1990 (Enge, 2020b). The lake was limed in the period 1990-2016, discussed in 2.5. The latest fish surveys in Hunnedalen watershed (Enge, 2016, 2018, 2019, 2020a, 2020b) found the pH Lake Djupavatn, measured in July, to be 5.5, 5.7, 5.7, 5.9, and 6.5 for 2020, 2019, 2018, 2017, and 2015, respectively.

The acidification in Rogaland county had returned to a stabilized state in the last two decades, where the water quality was close to the natural state (Enge, 2013).

2.4 Water regulation

In 1983 an area of 38,14 km^2 (*NVE (Noregs Vassdrags- Og Energidirektorat)*, n.d.) of the highest altitude area of the watershed was regulated to be utilized as hydropower (Figure 2-4). The water is pumped from Lake Hunnevatn, in Hunnedalen watershed, to Lake Gravatn,

in Sira watershed. This area, which included Lake Hunnevatn, corresponded to 36% of the total watershed (*NVE (Noregs Vassdrags- Og Energidirektorat)*, n.d.). An improved water quality was found in the downstream watershed in the following years after the lake regulation (Samdal, 1987).

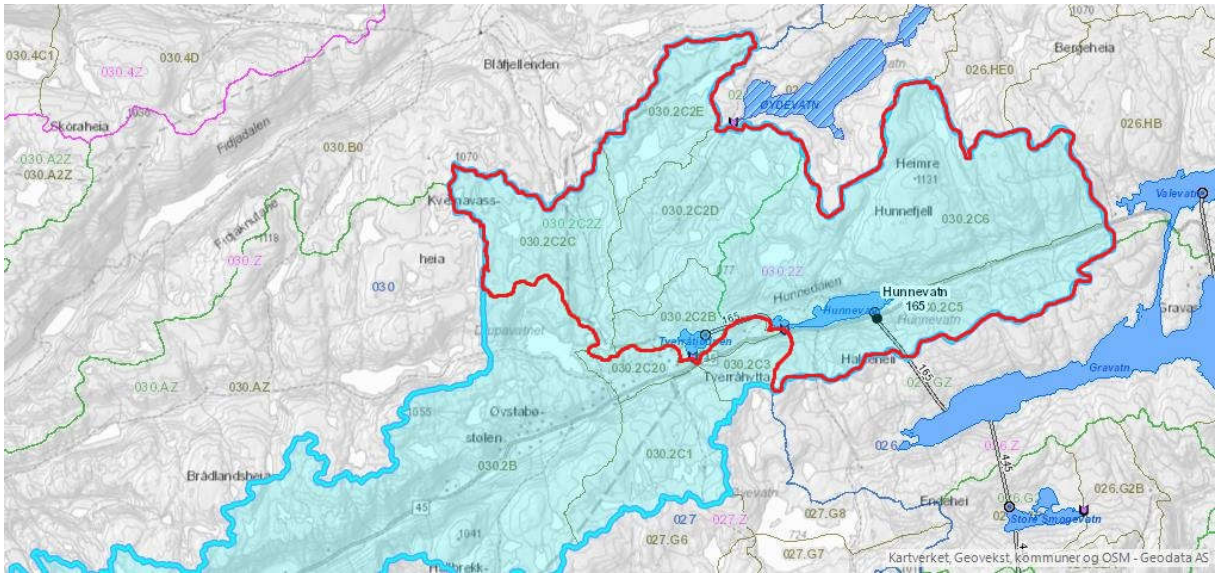

Figure 2-4 Highest altitude area of the watershed. The area affected by the lake regulated is outlined in red.

2.5 Liming

Lake Djupavatn, not a part of the regulated area, was limed annually from 1990 to 2016 (Enge, 2020b). The inlets to Lake Djupavatn was limed with carbonate sand up until 1998 (Ledje & Jastrey, 2006). Shortly after the first liming the lake was stocked with brown trout, further discussed in 2.6.

A fish- and water-chemistry survey was implemented to follow up the liming, measuring water quality twice a year and test fishing several times a during the period. After the termination of the liming, the fish- and water-chemistry survey was conducted annually. The latest survey, 30.06.20, concluded that the termination of liming was a correct discission, where no negative impacts on the fish population or water quality had occurred (Enge, 2020b).

2.6 Fish population and survivability

The fish species represented in the watershed are brown trout (*Salmo trutta*) and brook trout (*Salvelinus fontinalis*), where the latter is a foreign specie (Enge, 2005). Further, salmon (*Salmo salar)* is represented in the lowest altitude part of Hunnedalen river.

The native fish in the watershed went extinct or declined in the 1960-1970. After the water regulations in 1983, Sira-Kvina was imposed to stock the affected area with fish. Hence, brook trout was stocked. Brown trout from Hunnedalen river was stocked in Lake Hunnevatn (Enge, 2005).

Along with the liming of Djupavatn, 850 brown trout from Hunnedalen river was stocked in Lake Djupavatn in the period 1990 to 1996 (Ledje & Jastrey, 2006).

The water that got redirected out of the watershed was found to improve the downstream water quality the following years, explaining the survival of the brown trout in Hunnedalen river (Samdal, 1987). The state of Lake Djupavatn, with respect to brown trout density, was reported to be very good in period 1992-2020 with an exception of 2006 that was reported to be good (Enge, 2020b). The salmon population in the lower part of Hunnedalen river was reported to be stable with an increase of salmon angles in the period 2009-2020 (Enge, 2020b).

Although the watersheds in Rogaland may be recovered from the acidification from the early 1900's, dilute water quality and ion deficit were found to be the limiting factors for the brown trout population (Enge & Hesthagen, 2016). Recruitment of brown trout was found to be affected negatively by extreme low conductivity and calcium concentration during late snowmelt periods, in a neighbouring watershed (Enge, Hesthagen, et al., 2017). The opposite effect was found during sea salt deposition episodes, where an acceleration of brown trout recovery was found (Enge et al., 2016). Further, the effect of sea salt deposition are often negative, where mobilization of inorganic aluminum is of great concern (Teien et al., 2004, 2005). Brown trout survives in pH values above 4.5 (Jellyman & Harding, 2014), and mortality for salmon was found for pH values below 5.8 (Kroglund & Staurnes, 2011).

2.7 Anthropogenic activities

County road 45 follows Hunnedalen river through the entire watershed. The road is an alternative access road to eastern Norway, and the main access road to multiple cabin villages. The road was salted during winter, and patches of roadwork has been observed sporadically throughout the sampling period.

The watershed is affected by agricultural activity, with several farms with the highest altitude fields at 500 m a.s.l.. Further, sheep are grazing in the mountains during the summer months.

Two major cabin villages are located in the watershed, with 326 cabins combined (*Statistisk sentralbyrå (Statistics Norway)*, n.d.). Øvstabøstølen is lowest altitude cabin village in the watershed, located at ~550 m a.s.l.. The second village is within 4 km overhead line east of Øvstabøstølen, located at ~600 m a.s.l.. Most cabin activity happens during late winter and easter, or during summer.

These are all sources to possible contaminants to the watershed. Nutrients, such as phosphorous and nitrate, could potentially come from fertilizing, sheep excretes, hikers and cabin activity. Further, oils, salts, and contamination could come from roadwork, road maintenance, and cars.

3 Theory/Background

3.1 Atmospheric contribution and processes

3.1.1 Sea salt contribution

Many of natural water's main components has both a marine and non-marine origin. In different context it is important to separate these contributions. Non-marine cations represent alkalinity, whereas marine cations do not generate alkalinity. The marine contribution of an ion can be estimated by the relative composition of ocean water and the natural water's chloride concentration (Table 3-1). Chloride found in freshwater samples can be assumed to origin exclusively from the ocean. The non-marine contribution of each ion can be determined by using the following formula:

$$[X]^{*} = [X] - \left[\frac{X}{Cl^{-}}\right]_{sea} * [Cl^{-}]_{sample}$$

Subsequently, the marine contribution is determined by:

$$[X]^{**} = \left[\frac{X}{Cl^{-}}\right]_{sea} * [Cl^{-}]_{sample}$$

[X] is the total concentration of a ion in a given sample, [X]* is the nonmarine concentration of the given ion, $[X]^{**}$ is the marine contribution of the given ion, $[X/Cl^{-}]_{sea}$ is the proportion of the ion compared to chloride (Table 3-1), $[Cl^{-}]_{sample}$ is the chloride concentration in the sample.

Table 3-1 Primary ionic composition of sea water (Stumm & Morgan, 1995).

Ion	Seawater (g/kg)	Ratio to Cl^{-}
Na^{+}	10.77	0.556
Mg^{2+}	1.29	0.068
Ca^{2+}	0.41	0.02125
K^{+}	0.40	0.0206
Cl^{-}	19.35	0.9989
SO_4^{2-}	2.71	0.14

3.1.2 Precipitation chemistry

Water can be transported over long distances as gaseous water by air currents, further, to be deposited as rain or snow. While the water travels through the lower part of the atmosphere it can equilibrate with other gaseous components. The two major atmospheric constituents, N_2 and O_2, are only sparingly soluble in water, whereas CO_2 and SO_2 are very soluble (Snoeyink & Jenkins, 1980).

The pH in precipitation from an unpolluted atmosphere is 5.5-5.6, due to the CO_2 equilibrium (Snoeyink & Jenkins, 1980). Pollution such as SO_2 and NO_x originates from anthropogenic combustion. These compounds react with atmospheric water and oxygen to form sulfuric and nitric acid, which decreases the pH of the precipitation below 5.5 (Snoeyink & Jenkins, 1980).

A coastal gradient of marine contribution in the precipitation was found in southern Norway, with a decreasing ion concentration with distance from the coast (Wright & Henriksen, 1978). Hence, the marine contribution gradient was found to have a geographical distribution.

3.2 Water chemistry

3.2.1 Eutrophication

Eutrophication is a phenomenon in lakes caused by high nutrient loads in the influent rivers and brooks. This leads to an increased primary production in the epilimnion, causing a higher amount of biomass, which leads to a higher oxygen demand, oxygen depletion, in the hypolimnion (Ansari et al., 2011). Limiting nutrients are often nitrogen and phosphorous, where the latter is most common in freshwater bodies (Conley et al., 2009).

3.2.2 Hydrogeochemical contribution

Natural water bodies are highly dependent on the local conditions (Brezonik & Arnold, 2011), where the hydrogeochemical processes includes dissolution, precipitation, redox reactions, ion exchange, complexing and hydrolysis. Water and carbonic acid derived from the atmosphere acts as the primary source of weathering agents (Stumm & Morgan, 1995). CO_2 is protolyzed in two steps to form carbonic acid:

$$CO_{2(g)} \leftrightarrow CO_{2(aq)}$$

$$CO_{2(aq)} + H_2O \leftrightarrow H^+ + HCO_3^-$$

$$HCO_3^- \leftrightarrow H^+ + CO_3^{2-}$$

Calcite being a prime example of such weathering process.

$$CaCO_3 + H^+ \leftrightarrow Ca^{2+} + HCO_3^-$$

$$CaCO_3 + H_2O \leftrightarrow Ca^{2+} + HCO_3^- + OH^-$$

$$CaCO_3 + H_2O + CO_2 \leftrightarrow Ca^+ + HCO_3^-$$

This reaction represents many different weathering reactions, where alkalinity is often generated. Some rock types, on the other hand, consume alkalinity. Such example could be pyrite (FeS_2) (Gu et al., 2020; Stølen, 2019). Further, some rock types are slow weathered, leading to a low buffer capacity in the surface water. Among these slow weathered rock types are gneiss.

3.2.3 Alkalinity and acidification

Alkalinity is the waters capacity to neutralize strong acids. Carbonate, bicarbonate and OH^- are the most important parameters when it comes to natural waters. Other ions such as ammonia, phosphates, borates, aluminum, and organic acids can also affect or contribute to this capacity (Snoeyink & Jenkins, 1980), where aluminum and organic acids are of interest in Hunnedalen watershed. Due to the latter parameters' low contribution relative to the carbonate buffer, the general formula can be expressed on this form:

$$[ALK] = [HCO_3^-] + 2[CO_3^{2-}] + [OH^-] - [H^+]$$

The equilibrium of atmospheric and dissolved CO_2 yields a pH of 5.5-6.5 in "unpolluted" precipitation (Snoeyink & Jenkins, 1980). Therefore, $[CO_3^{2-}]$ and $[OH^-]$ can be neglected. $[H^+]$ is also relatively small, and the alkalinity can be estimated to be:

$$[ALK] \approx [HCO_3^-]$$

The carbonate buffer system's first dissociation stage is given by the expression:

$$\frac{[H^+][HCO_3^-]}{[CO_{2(aq)}]} = K_{a1}$$

pK_{a1} is given to be 6.35 (Stumm & Morgan, 1995), and the equilibrium concentration of CO_2 in water at (25 C) is given to 10^{-5}M (Hongve, 1982). The pH can be estimated to be:

$$pH = 11.35 + \log [HCO_3^-]$$

Further, oligotrophic lakes are generally oversaturated or supersaturated with CO_2 (Norton & Henriksen, 1983).

Direct use of the endpoint titration yields an overestimation of the true equivalence alkalinity for samples with low alkalinity (Snoeyink & Jenkins, 1980). To adjust for overestimation, the equivalence alkalinity formula, ALK_e, was used (Henriksen, 1982).

$$ALK_e = ALK_{pH=4.5} - 32 + 0.646 * \sqrt{ALK_{pH=4.5} - 32}$$

The acid-neutralizing capacity, ANC, is an alternative definition of alkalinity and takes the wide range of proton-accepting and proton-donating species into account. The estimation is often simplified to only contain strong cation and strong acid anions.

$$ANC = \sum(proton\ acceptors) - \sum(proton\ donors)$$

$$ANC = [Ca^{2+}] + [Mg^{2+}] + [Na^+] + [K^+] - [SO_4^{2-}] - [Cl^-] - [NO_3^-]$$

The weathering of bedrock produces equivalent amount of alkalinity and cations (Wright & Henriksen, 1978). Further, in water bodies with a low concentration of organic compounds, the alkalinity is approximately equal to the ANC.

Acidification is defined as a loss of alkalinity and can be estimated by the difference between pre-acidification, the original alkalinity, and the current alkalinity (Henriksen, 1980).

$$ANC = [ALK]_{loss} = [ALK]_0 - [ALK]$$

The original alkalinity, $[ALK]_0$, can be estimated as the sum of the non-marine cations, marked with asterisk. It is approximately equivalent to the sum of non-marine calcium and magnesium. Simpler equations have also been proposed (Henriksen, 1980).

$$[ALK]_0 \approx 0.91 * ([Ca]^* + [Mg]^*)$$
$$[ALK]_0 \approx 1.21 * [Ca]^*$$

Due to acidification, the measured alkalinity, [ALK], will be lower compared to the original alkalinity, $[ALK]_0$. This is caused by natural acidification (SO_4 that originates from volcanoes or oxidation of sulfides) or anthropogenic acidification (SO_4 and NO_x from combustion processes).

$$[ALK] = [ALK]_0 - \sum acidification$$

4 Methods

4.1 Sample preparation

Samples from a total of 10 locations was sampled. Eight of the samples were collected monthly, directly or in near relation to Hunnedalen river. These samples will be referred to as Gilja, Byrkjedal, VM Byrkjedal (limnigaph station), Øvstabø river, Øvstabø brook, Djupavatn brook, Hunnevatn outlet and Hunnemonen (Figure 4-1). The respective location's altitudes were 55, 360, 238, 500, 565, 605, 650 and 655 m above sea level. Byrkjedal was acting as a reference sample for the lower altitude area of the watershed. Two lakes were sampled at 0m, 5m, 10m, and 20m depth every other month, and will be referred to as Lake Djupavatn and Lake Hunnevatn (Figure 4-1). The lakes altitudes were 711 m and 650 m above sea level, respectively. Two logging devices, measuring conductivity and temperature, were placed at VM Byrkjedal and Hunnemonen (Figure 4-1).

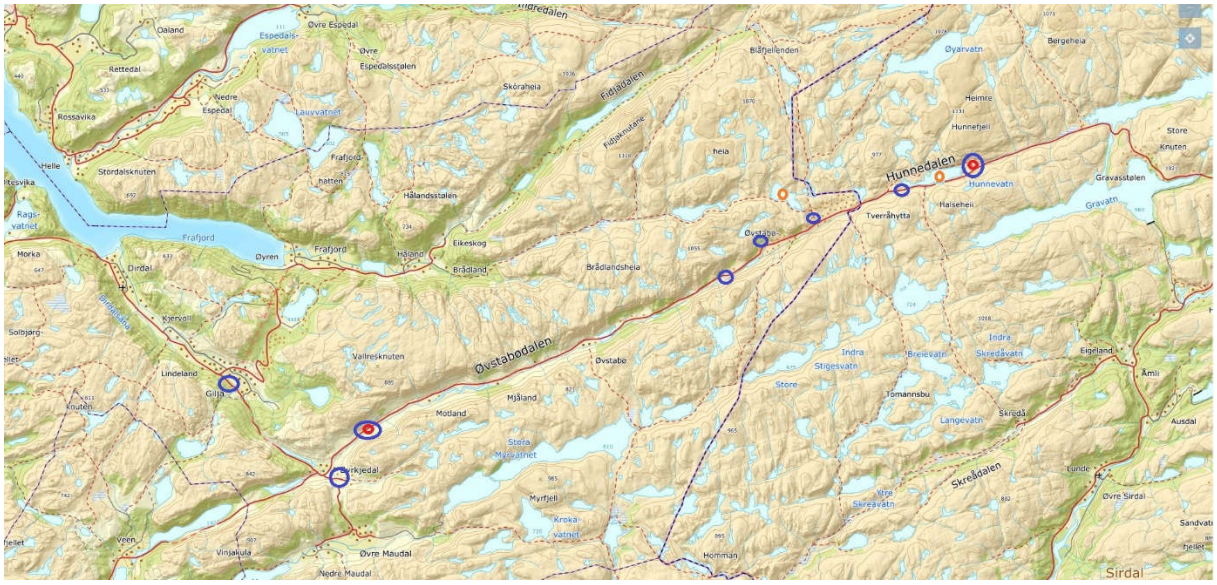

Figure 4-1 Map of Hunnedalen watershed with sampling locations marked as circles. Blue circles (in relation to Hunnedalen river): Gilja, Byrkjedal, VM Byrkjedal, Øvstabø river, Øvstabø brook, Djupavatn brook, Hunnevatn outlet, Hunnemonen (left to right). Orange circles (lake samples): Lake Djupavatn, Lake Hunnevatn (left to right). Red circles (logging devices): VM Byrkjedal, Hunnemonen (left to right).

4.2 Analytical methods

A total of 15 parameters was determined for a total of 156 samples. Temperature was only measured for the lake samples. Further, sulfate and magnesium were only determined for Byrkjedal, VM Byrkjedal and lake samples.

Non-preservable parameters, color, pH, conductivity, and alkalinity was measured within 48 hours of sampling.

Dissolved phosphorous was determined from November 2019 to February 2020, whereas total phosphorous was determined for the remaining samples. This was due to covid-19 and laboratory restrictions, and samples were acid conserved for the total phosphorous determination.

Frequently-used methods for determination of the parameters measured was not used, due to lack of required instrumentation.

4.2.1 pH

pH was measured potentiometrically according to "The Standard Methods" 4500-H^+ pH Value (Eaton et al., 1998). A Cole Parmer pH meter with a Radiometer pHC4001 electrode was used. Standard buffers of pH 4.01 and pH 6.86 was used as calibration.

4.2.2 Alkalinity

Alkalinity was determined by titration with 0.0025 N H_2SO_4. By interpolation of the titration curve, the titration volume corresponding pH=4.5 was determined. Direct use of this endpoint yields an overestimation of the true equivalence alkalinity for samples with low alkalinity (Snoeyink & Jenkins, 1980). To adjust for over-titration, the equivalence alkalinity formula, ALKe, was used (Henriksen, 1982).

$$ALK_e = ALK_{pH=4.5} - 32 + 0.646 * \sqrt{ALK_{pH=4.5} - 32}$$

4.2.3 Conductivity

Conductivity was determined according to "Standard Methods" 2510 (Eaton et al., 1998), using Amber Science mod. 1056 conductivity meter

4.2.4 Calcium

Calcium was measured potentiometrically using a Radiometer ISE25Ca Electrode. A Ref201 single junction electrode saturated with KCl was used as a reference electrode. The samples were prepared with an ISA, adding 0.1 M KCl to each sample.

4.2.5 Chloride

Chloride was measured potentiometrically using Radiometer ISE/HS25 Cl Electrode. A VWR double junction electrode was used as a reference electrode with 0.1 M KNO3 in the outer chamber. The samples were prepared with an ISA, adding 0.1 M KNO_3 to each sample.

4.2.6 Sodium

Sodium was measured potentiometrically using Radiometer ISE21NA Electrode. A Ref201 single junction was used as a reference electrode. To each sample of 10 ml, 5 ml ISA was added. The ISA consisted of 7.5 % ethanolamine adjusted to pH 10 with HNO_3.

4.2.7 Potassium

Potassium was measured potentiometrically using a Sentek electrode. A VWR double junction was used as a reference electrode with 0.1M NaCl in the outer chamber. The samples were prepared with an ISA, adding 0.1 M NaCl to each sample.

4.2.8 Magnesium

Magnesium was measured spectrophotometrically according to Ingman and Ringbom (1966).

4.2.9 Aluminum

Aluminum was measured photometrically according to "The Standard Methods" 3500-Al B Eriochrome Cyanine R (Eaton et al., 1998). To determine the labile aluminum, a sodium cation exchanger (Amberlite IR120 Na^+) was used. Transmission was measured at 530 nm with a HACH spectrophotometer in 1" plastic square cuvettes.

4.2.10 Sulfate

Sulfate was determined by conductometric titration with barium acetate, according to Stølen (2019), using a Greisinger GLF 100RW conductometer. The samples were pretreated by a sodium cation exchanger (Amberlite IR120 Na^+) to eliminate interferences from divalent cations. Isopropanol was added (v/v = 2:1) to reduce the solubility of $BaSO_4$. By recording the titration curve, a linear segment before and after the equivalent point were found. The volume was determined by the interception of the two linear segments using linear regression.

4.2.11 Phosphorous

Due to laboratory lockdown as of Covid-19, samples were conserved with acid to preserve for total phosphorous analysis. Therefore, dissolved phosphorous was only determined for the first months and total phosphorous was determined for the remaining months.

4.2.11.1 Dissolved phosphorous

Dissolved phosphorous was measured photometrically according to “The Standard Methods” 4500-P E Ascorbic Acid Method (Eaton et al., 1998), using an VWR UV-1600PC spectrophotometer.

4.2.11.2 Total phosphorous

The samples were conserved with 3 drops concentrated sulfuric acid to 125ml sample. The samples were prepared according to “The Standard Methods” 4500-P B 5. Persulfate Digestion Method (Eaton et al., 1998). An autoclave was used, with a max temperature at 121 C lasting 30 minutes. Further, phosphorous was measured photometrically according to “The Standard Methods” 4500-P E. Ascorbic Acid Method (Eaton et al., 1998), using an VWR UV-1600PC spectrophotometer.

4.2.12 Nitrate

Nitrate for all the samples was measured with a polymer membrane ion-selective electrode, Radiometer ISE25NO3, according to the user manual. Nitrate ion selective electrodes, in general, has a linear range of typical 5-200 mg/l, and nitrate concentrations below this limit will be biased high (EPA publication SW-846, 2015). Two modifications to the user manual were performed; firstly, $(NH_4)_2SO_4$ was used as ISA. Secondly, to assure the nitrate concentration was within the linear range of the electrode, 0.95 mg/l was added to every sample. The inner solution following the electrode was diluted 1:10, due to assumably low concentration of nitrate (Mikhelson, 2013).

4.2.13 Color

Color was determined according to NS 4722. Samples was analyzed unfiltered at 445 nm in 4 cm cuvettes with a Shimadzu spectrophotometer (UV-20-01).

4.3 Quality control

4.3.1 Precision and accuracy

Table 4-1 Overview of quality control analysis.

Parameter	Internal standard	Precision
pH	Distilled water	
Alkalinity	Certified reference	
Conductivity	Distilled water	
Calcium	Diluted sea water	
	Certified standard	
Chloride	Diluted sea water	
Sodium	Diluted sea water	
	Certified reference	
Magnesium	Diluted sea water	
Aluminum	Certified standard	Duplicates
Sulfate	Diluted sea water	
Phosphorous	Calibration controls	

General verification of the methods and instruments was controlled using internal standards, certified references and measuring duplicates.

Distilled water was measured for each session when pH and conductivity was measured. Calibration solutions was measured about every 5^{th} sample for calcium, chloride and sodium, whereas an internal standard was measured every 20^{th} sample. For aluminum, one duplicate and one internal standard was measured every 8^{th} sample. Phosphorous had one internal standard each 15^{th} sample.

Nitrate ion selective electrode in natural water is a disputed method of analyzing nitrate, where some considered the technique as highly unreliable (Raikos et al., 1988). A case study (Appendix A) was conducted where ion selective electrode and colorimetric determination of nitrate was statistically compared. pH, conductivity, color, alkalinity, chloride, nitrate with ion selective electrode, and colorimetric nitrate was determined for 44 samples. Some of the samples were spiked with Na_2SO_4, KNO_3, $NaHCO_3$ and seawater to extend the concentration ranges. Colorimetric nitrate was found to highly correlate with nitrate with ion selective electrode, color, alkalinity, conductivity, and chloride (R^2=0.96, $F_{5,38}$=204.10, p<0.001, n=44):

$$NO_3 \approx 0.84 * NO_3(ISE) - 2.0 * Color - 2.7 * ALK_e + 7.4 * Cond - 28 * Cl - 11$$

The estimated nitrate concentration was found to have an uncertainty of 55 µg/l. All the regression coefficients were individually significant ($p<0.001$). This formula was applied to all nitrate results yielded from nitrate ion selective electrode.

Duplicates of a random selection of aluminum samples was measured to test the precision of the analysis. The duplicates were statistically controlled by t-test, to further evaluate if the duplicates where significantly different or not.

4.3.2 Correctness of analysis

Snoeyink and Jenkins (1980) stated that the cation-anion balance for fresh water was ±2%. Further, a more common criterion for the cation-anion balance in oligotrophic lakes was ±10%.

The measured conductivity was compared to the calculated conductivity, with a criteria of ±10% according to "Standard Methods 1030 E" (Eaton et al., 1998).

4.4 External data

Weather data was gathered from the Meteorological institution of Norway (*MET (Meteorological Institute)*, n.d.), from the stations Maudal in Gjesdal, Rogaland, and Sinnes in Sirdal, Vest-Agder. Data from Djupavatn, as a part of Fylkesmannen's liming project, was gathered from Hunnedalen Association. Average runoff data and precipitation data was retrieved from nve.no (*NVE (Noregs Vassdrags- Og Energidirektorat)*, n.d.). Daily measurements of water flow at VM Byrkjedal limnigraph was retrieved from Sira-Kvina.

Fish and water chemistry data has been retrieved from "Fiskeundersøkelser I Rogaland", that covers the lower altitude parts of Hunnedalen river and Lake Djupavatn for the five last years (Enge, 2016, 2018, 2019, 2020a, 2020b).

4.5 Simulation of calcium

Simulation of non-marine calcium was done by estimating non-marine calcium flux (g/s) as a function of runoff (m^3/s) at VM Byrkjedal and for the regulated area. Non-marine calcium was estimated, as discussed in 3.1.1. The runoff data used was measured at VM Byrkjedal limnigraph. An estimation of the total regulated area's runoff was made by the annual average ratio of the runoff at VM Byrkjedal and the regulated area (*NVE (Noregs Vassdrags-*

Og Energidirektorat), n.d.). The regulated area's runoff was estimated to be 72.9% of VM Byrkjedals runoff. Linear regression was applied to find the calcium flux and runoff relation of the two water bodies.

4.6 Statistical methods

Microsoft Excel 2016 was used for all the statistical work. Paired t-test was used for analyzing significant difference between duplicates for quality control. Multiple regression was used to analyze significant relationship between variables. Multiple regression was also used for modeling of pH, where backwards elimination was preformed until all predictors were significant ($p < 0.05$).

4.7 Original pH

Original pH was estimated using "Opprinnelig regneark.XLS" (Hindar & Wright, 2002). This Excel file estimates the original pH before the acidification, about 120 years ago. pCO_2 was set to 4 times the atmospheric partial pressure (Enge, 2009).

5 Results

5.1 Quality control

5.1.1 Precision and accuracy

All parameters controls showed both a high accuracy and a good precision (Table 5-1). Replicate pH and conductivity measurements of distilled water showed high precision (pH = 5.55 ± 0.04, n=13 | Conductivity = 1.4 ± 0.1, n=12).

Table 5-1 Control determinations.

Parameter	Known concentration (mg/l)	n	Average	Standard deviation
Alkalinity	96.1**	10	103.4**	2.63**
Calcium	0.32	27	0.34	0.03
	4.8	20	4,84	0.10
Chloride	3.86	28	3.81	0.06
Sodium	2.14	35	2.13	0.04
	4.42	10	4.40	0.06
Magnesium	0.21	5	0.21	0.01
Aluminium	60*	9	61,9*	1,92*
Sulfate	1.73	5	1.73	0.08
Phosphorous	25*	5	26.12*	0.64*

*= µg/l

**= µeq/l

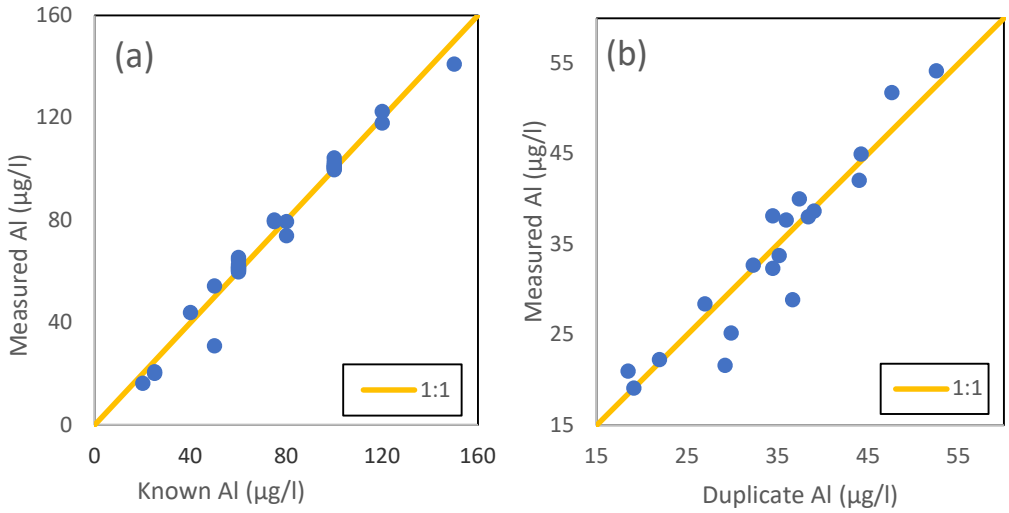

Figure 5-1 (a) Internal standards results from the aluminum analysis (µg/l). (b) Duplicates of random aluminum samples, where each sample was plotted against its duplicate (µg/l).

The aluminum control yielded a high correlation (R^2=0.97, STD=5 µg/l, n=29, p<0.05), where the precision of the 60 µg/l control was found to be 62±2 µg/l (n=9) (Figure 5-1, a). Duplicate

measurements of aluminum gave an equivalently good correlation (R^2=0.89, STD=3 µg/l, p<0.05, n=19), where no significant difference in the duplicates was found (Figure 5-1, b).

Validation of nitrate was further discussed in Appendix A and yielded a reliable concentration of the measurements with an uncertainty of ±55 µg/l. Ranges of the parameters measured were within the acceptable range of the validation of the case study's parameter ranges.

5.1.2 Correctness of analysis

The cation-anion balance was within the acceptable limit of ± 10% for all individual samples (R^2=0.99, n=71, p<0.05) (Figure 5-2, a). Further, 94% and 66% of the individual samples' cation-anion balance was within a limit of ±5% and ±2%, respectively.

The calculated conductivity showed a good precision compared to the measured conductivity (R^2=0.99, n=71, p<0.001) (Figure 5-2, b).

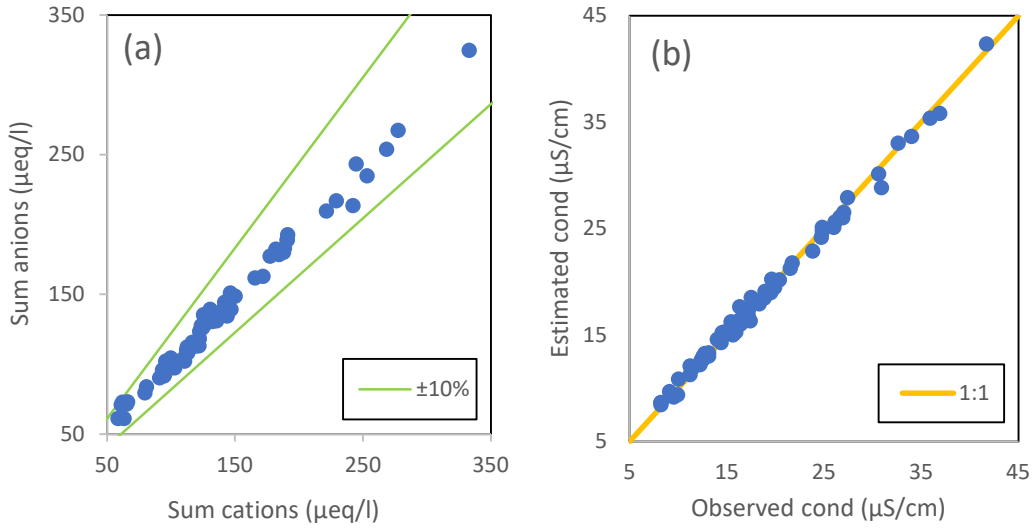

Figure 5-2 (a) Cation-anion balance for every individual sample (µeq/l). The green lines represent the ±10%. (b) Estimated conductivity (µS/cm) for every individual sample plotted against the observed conductivity (µS/cm).

5.2 Water chemistry

The annual averages of Hunnedalen watershed, excluding Byrkjedal, shows a decreasing pH and conductivity with increasing altitude (Table 5-2). The annual average chloride and sodium concentrations had a significant correlation with the altitude of the samples (Figure 5-3, a, b). A decrease of 0.0024 mg/l and 0.0016 mg/l was found per meter above sea level, for chloride and sodium respectively (Cl: R^2=0.87, n=8, p<0.001 | Na: R^2=0.92, n=8, p<0.001).

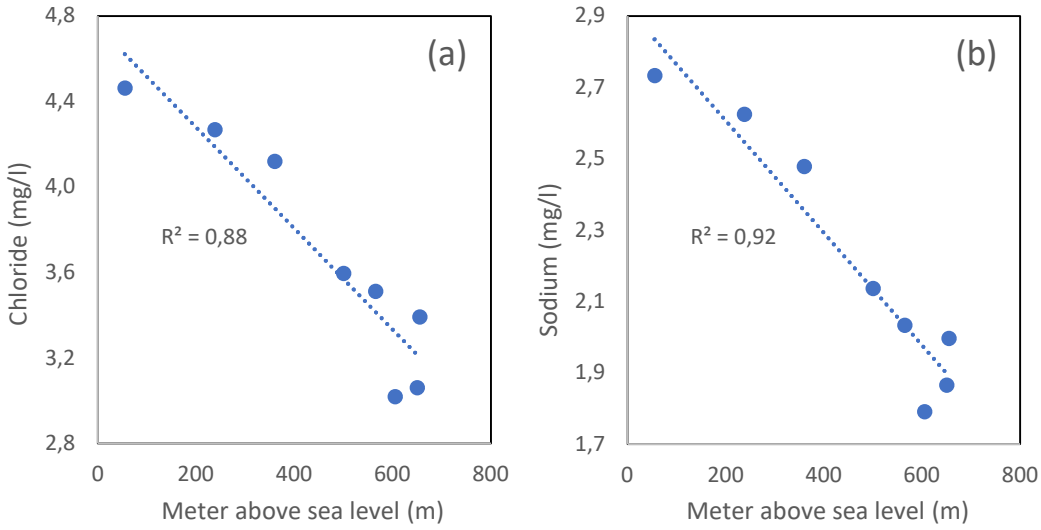

Figure 5-3 Annual average chloride (mg/l) and sodium (mg/l) concentration of the different location, plotted against the location's altitude (m). (a) chloride (mg/l) against altitude (m a.s.l.). (b) sodium (mg/l) against altitude (m a.s.l.).

Byrkjedal, acting as a reference, showed a significantly lower pH and ALK_e, and higher Al and LAl compared to the samples of Hunnedalen watershed (Table 5-2). Hunnevatn outlet has somewhat higher pH, ALK_e and Ca^{2+} compared to the other sampling locations.

Total phosphate was below limit of detection (<3 µg/l) for all but one sample (Byrkjedal, 07.02.20, 3 µg/l).

Table 5-2 Annual average water chemistry for each sampling location, November 2019 to December 2020.

Location	m a.s.l.	n	pH	Conductivity	Colour	ALKe	K	Ca	Cl	Na	Mg	Al	LAl	SO4	NO3	Tot-P
	m			µS/cm	mg Pt/l	µeq/l	mg/l	mg/l	mg/l	mg/l	mg/l	µg/l	µg/l	mg/l	µg/l	µg/l
Gilja	55	13	5,91	22,9	17	18	0,24	0,57	4,5	2,7		36	10		194	<3
Byrkjedal	360	14	5,49	21,4	23	7	0,14	0,37	4,4	2,6	0,30	46	14	1,35	97	<3
Vm byrkjedal	238	15	5,91	23,0	15	17	0,19	0,59	4,5	2,7	0,32	33	9	1,40	205	<3
Øvstabø river	500	13	5,63	18,3	16	10	0,19	0,34	3,6	2,1		36	12		103	<3
Øvstabø brook	565	13	5,43	17,2	12	4	0,17	0,27	3,5	2,0		40	18		98	<3
Djupvatn brook	605	13	5,62	15,3	20	10	0,16	0,28	3,0	1,8		39	11		78	<3
Hunnevatn outlet	650	13	5,81	17,6	14	33	0,20	0,63	3,1	1,9		40	14		118	<3
Hunnemo	655	14	5,57	16,9	9	9	0,18	0,30	3,3	1,9	0,22	45	25	0,95	113	<3
Lake Hunnevatn*	650	24	5,42	17,3	15	6	0,18	0,25	3,4	2,0	0,25	45	21	0,98	95	<3
Lake Djupavatn*	711	24	5,56	15,1	19	11	0,16	0,28	2,9	1,7	0,22	38	11	0,98	65	<3

*= Averages of all depths.

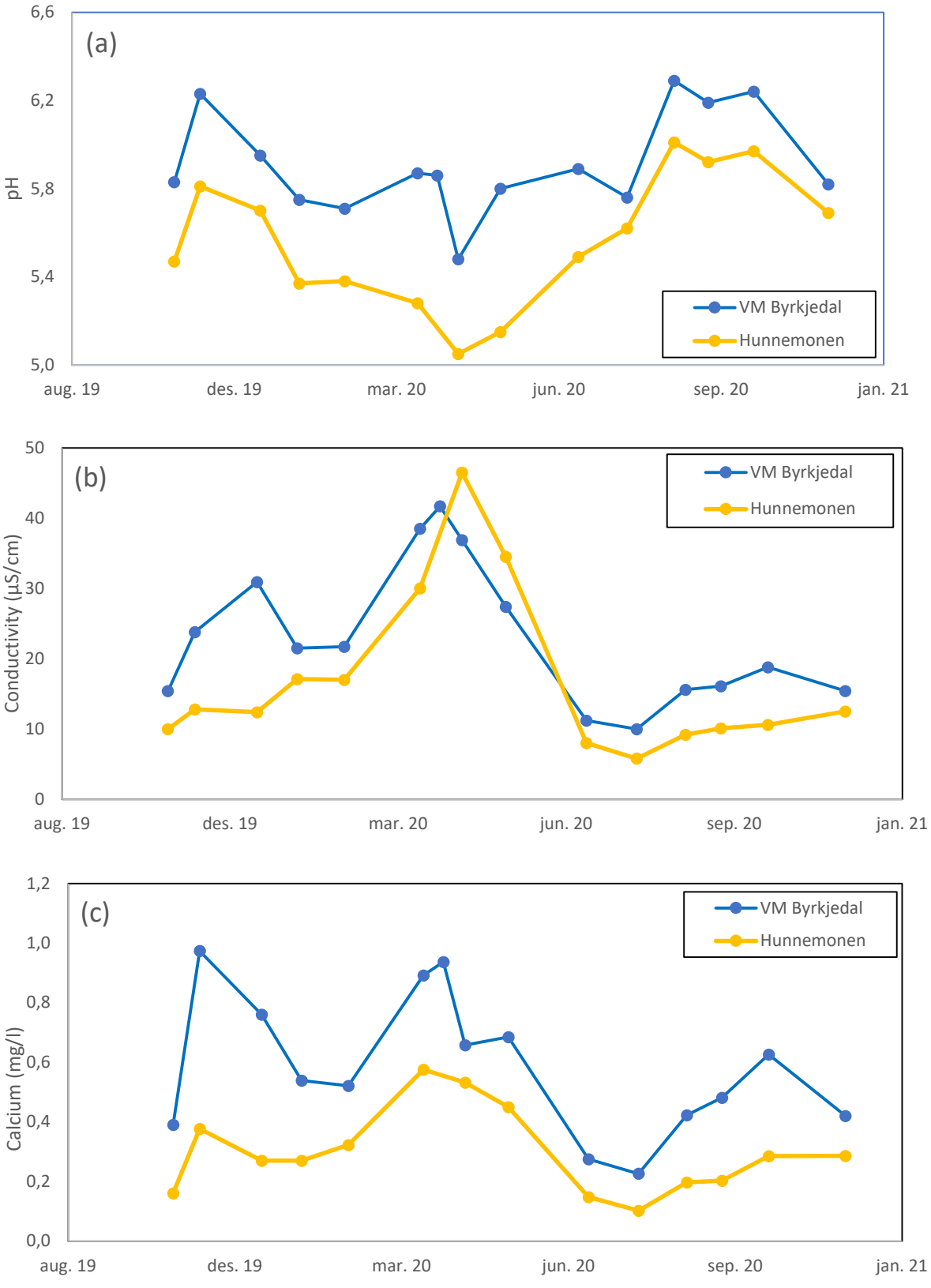

Figure 5-4 (a) Annual profile of pH at VM Byrkjedal and Hunnemonen. (b) Annual profile of conductivity (µS/cm) at VM Byrkjedal and Hunnemonen. (c: Annual profile of calcium (mg/l) concentration at VM Byrkjedal and Hunnemonen.

The annual profile for pH shows a lower pH from March 2020 to May 2020, and a higher pH in November 2019 and from august 2020 to November 2020 (Figure 5-4, a). The same trend was found for the conductivity profile, but reversed (Figure 5-4, b). The calcium profile correlated to the conductivity profile somewhat, where both parameters are increased from March 2020 to May 2020 (Figure 5-4, c).

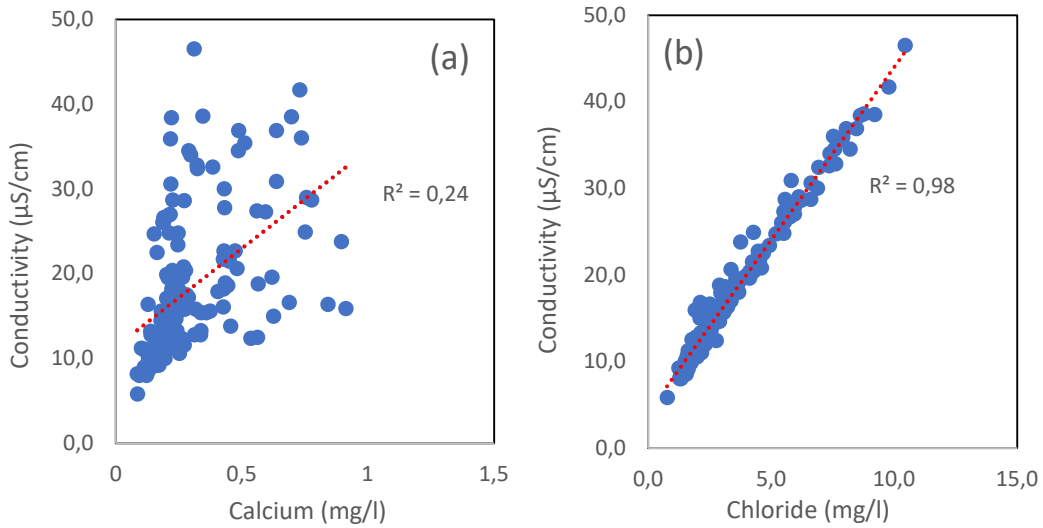

Figure 5-5 (a) Conductivity (µS/cm) plotted against chloride (mg/l). (b) Conductivity (µS/cm) plotted against non-marine calcium (mg/l) for every. All samples were individual samples.

The annual conductivity profile does not strictly follow the annual calcium profile. There was found some relation between conductivity and non-marine calcium (n=156, R^2=0.24) (Figure 5-5, a). Further, a clear correlation between chloride and conductivity was found (n = 156, R^2=0.98) (Figure 5-5, b), which suggests that the conductivity is highly dominated by the marine contribution.

Inorganic aluminum was found to correlate with conductivity at a different degree for the different locations. The locations VM Byrkjedal, Gilja and Djuapavatn brook, was found to have a less significant and weaker correlation between the two parameters (R^2=0.21, n=41, p<0.05). Whereas Byrkjedal, Øvtasbø brook, Øvstabø river, Hunnevatn outlet, Hunnemonen, Lake Djupavatn and Lake Hunnevatn, were the locations found with the strongest correlation (R^2=0.66, n=115, p<0.001). Especially, the correlation at Hunnemoen was found to be very strong (R^2=0.93, n=14, p<0.001), where the two annual profiles are close to identical (Figure 5-6).

The inorganic ratio of aluminum found to correlate well with measured alkalinity linearly and color logarithmically (n=153, $F_{2, 151}$=78.26, R^2=0.50, p<0.001).

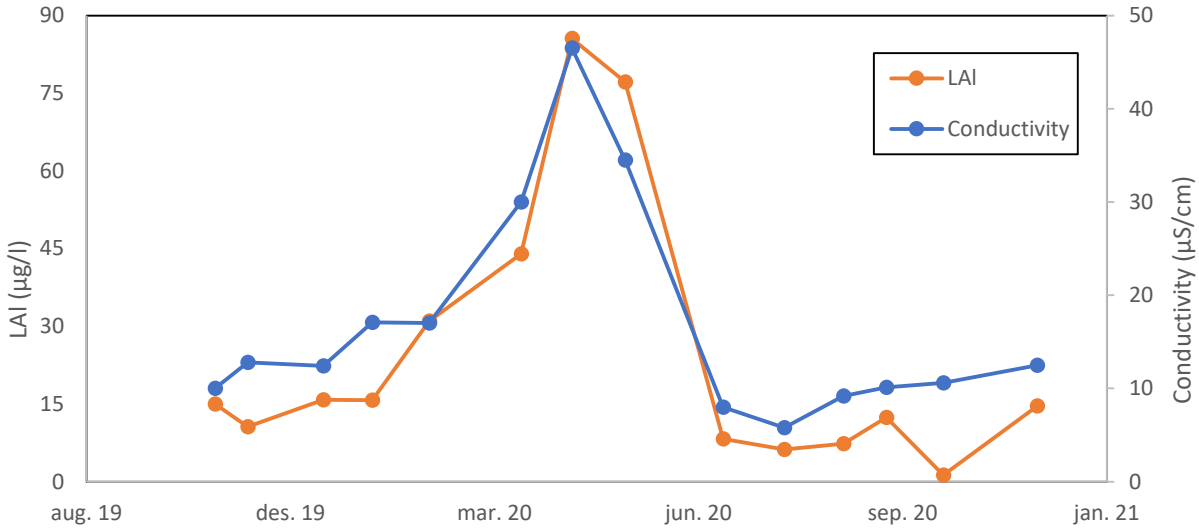

Figure 5-6 Annual profile of Lal (mg/l) and conductivity (µS/cm) at Hunnemonen.

The estimated alkalinity loss, $[ALK]_{loss}$, was estimated, and all stations except Hunnevatn outlet yielded a significant alkalinity loss. An annual ratio of 0.21 to 0.66 of the estimated original alkalinity, $[ALK]_0$, was consumed for the all stations. At Hunnevatn outlet an annual ratio of 0.03 was found (Figure 5-7, a). The average alkalinity loss was also estimated at each date, using averages of all stations (Figure 5-7, b). A relatively high alkalinity loss was found from October 2019 to May 2020, with a ratio of 0.33 to 0.70. A lower alkalinity loss was found from April 2020 to December 2020, with a ratio of 0 to 0.19.

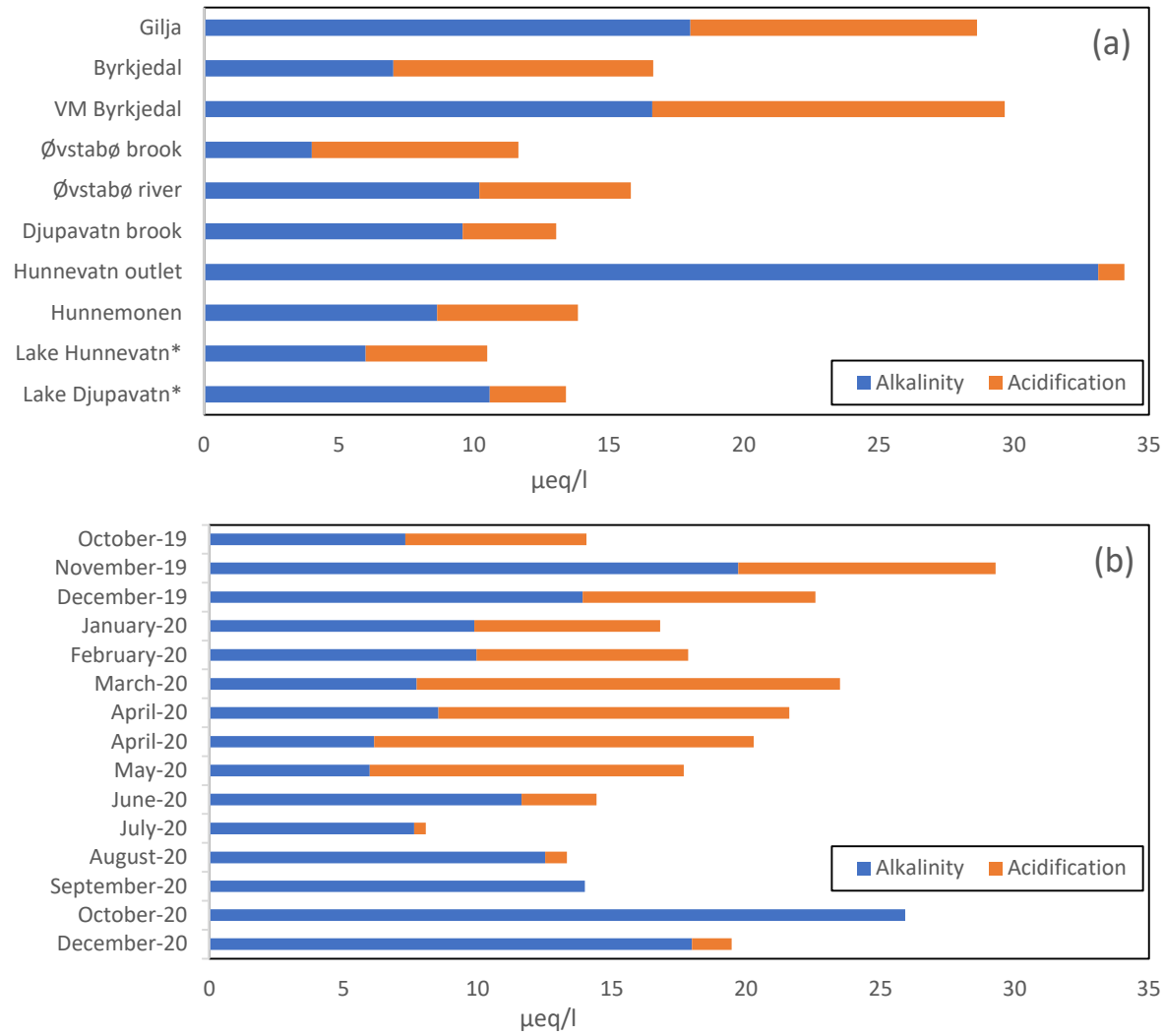

Figure 5-7 Estimated acidification for annual averages for locations (a) and date averages for all locations (b). Equation 1.21x[Ca] (Henriksen, 1980) was used for the original alkalinity estimation $[ALK]_0$. The total bars represent estimated original alkalinity, $[ALK]_0$.*

The analysis conducted of the two lakes showed a winter stratification from January to May (Figure 5-8, a-g). Further, in the period from May to the end of June, Lake Djupavatn had mixed and stabilized summer stratification (Figure 5-8, h). The summer stratification is not stabilized for Lake Hunnevatn in July (Figure 5-8, i). The summer stratification is visible through August, but the lakes are mixed for the remaining months of September and October (Figure 5-8, (j)-(l)). The pH yields an equivalent depths gradient as conductivity, only reversed.

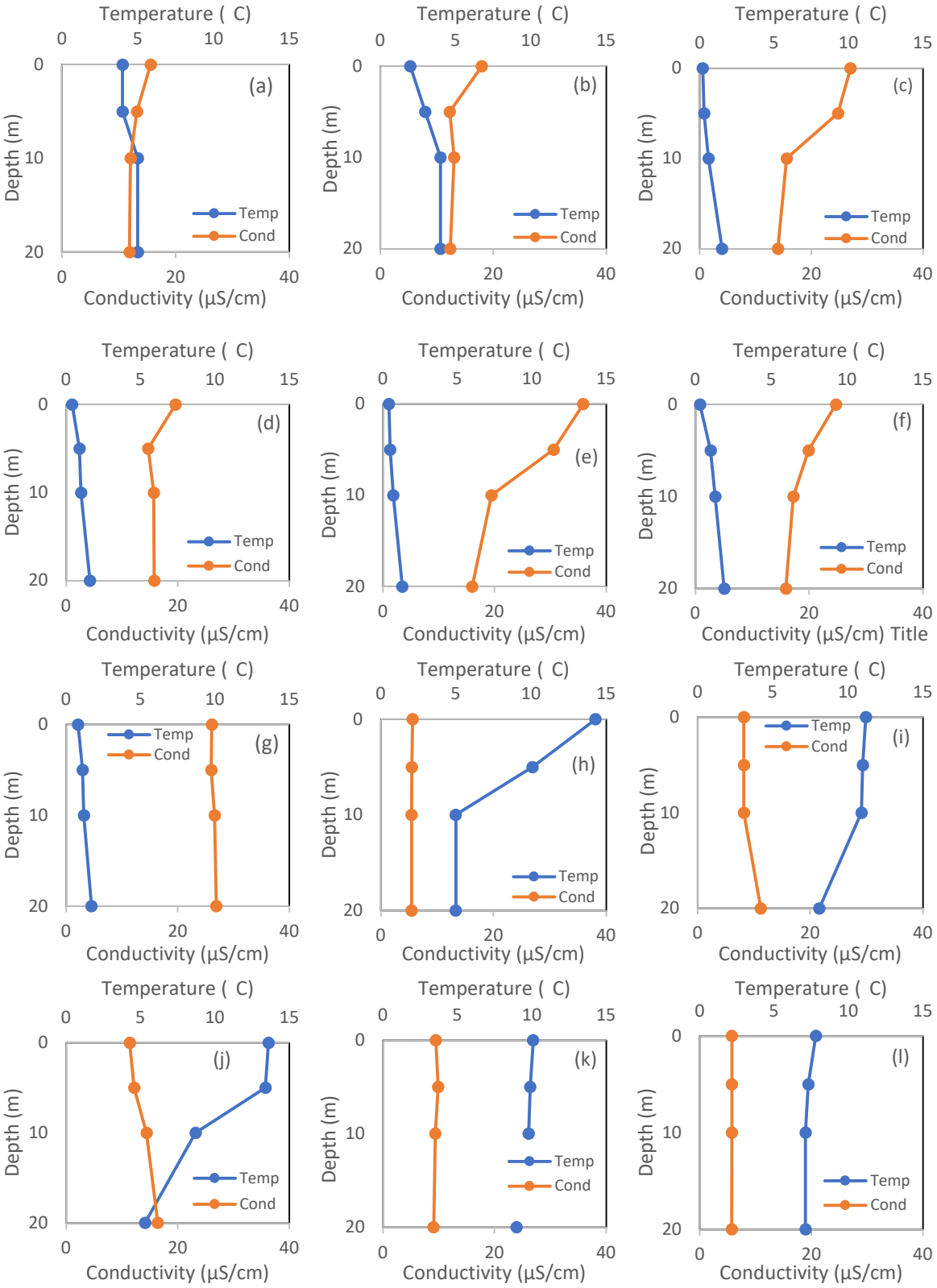

Figure 5-8 Depths profile for all lake samples. Y-axis represents depths. Primary x-axis represents conductivity (µS/cm), and secondary x-axis represents temperature (C). (a) Lake Hunnevatn 10.01.20. (b) Lake Djupavatn 07.02.20. (c) Lake Hunnevatn 23.03.20. (d) Lake Djupavatn 04.04.20. (e) Lake Hunnevatn 17.04.20. (f) Lake Djupavatn 13.05.20. (g) Lake Hunnevatn 13.05.20. (h) Lake Djupavatn 30.06.20. (i) Lake Hunnevatn 30.07.20. (j) Lake Djupavatn 28.08.20. (k) Lake Hunnevatn 18.09.20. (l) Lake Djupavatn 16.10.20.

5.3 Modelling and simulations

5.3.1 Calcium model

Water quality at VM Byrkjedal represents the water chemistry downstream to the lake regulation. Further, water quality at Hunnemonen represents the water quality of the regulated area. Significant correlations were found between calcium flux and runoff data (Figure 5-9, a, b).

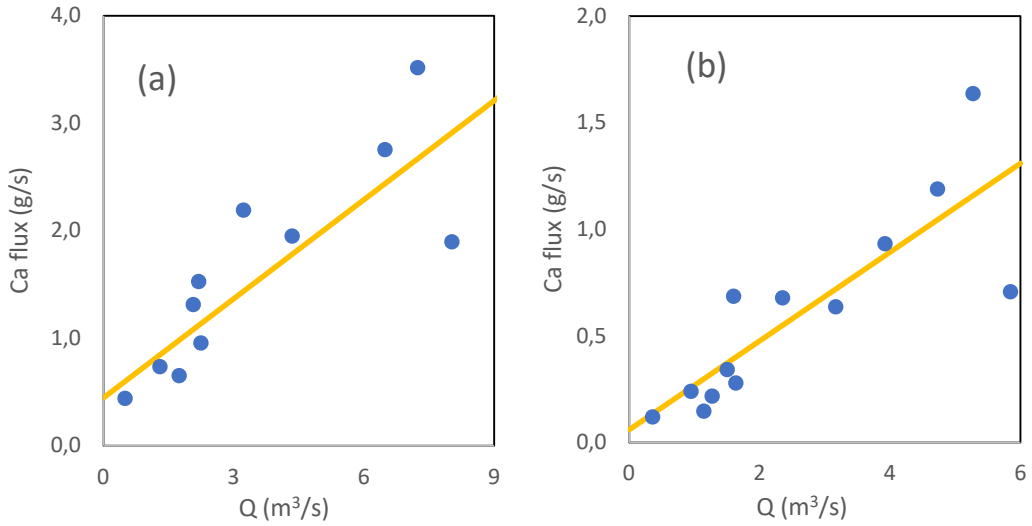

Figure 5-9 Calcium flux (g/s) as a function of water flow (m³/s) at (a) VM Byrkjedal and (b) Hunnemonen. Regression line is shown with a yellow line.

$$VM\ Byrkjedal: J_{Ca} = 0.45 + 0.31Q_{VMBy}\ (R^2 = 0.74, p < 0.001, n = 11)$$

$$Regulated: J_{Ca} = 0.06 + 0.21Q_{Regulated}\ (R^2 = 0.70, p < 0.001, n = 13)$$

The calcium concentration in terms of waterflow in the unregulated river can be expressed as follows:

$$Ca_{mix} = \frac{1}{Q_{tot}} * \left(J_{Ca-VMBy} + J_{Ca-Regulated}\right)$$

$$Ca_{mix} = \frac{1}{Q_{tot}} * \left(0.51 + 0.31Q_{VMBy} + 0.21Q_{Regulated}\right)$$

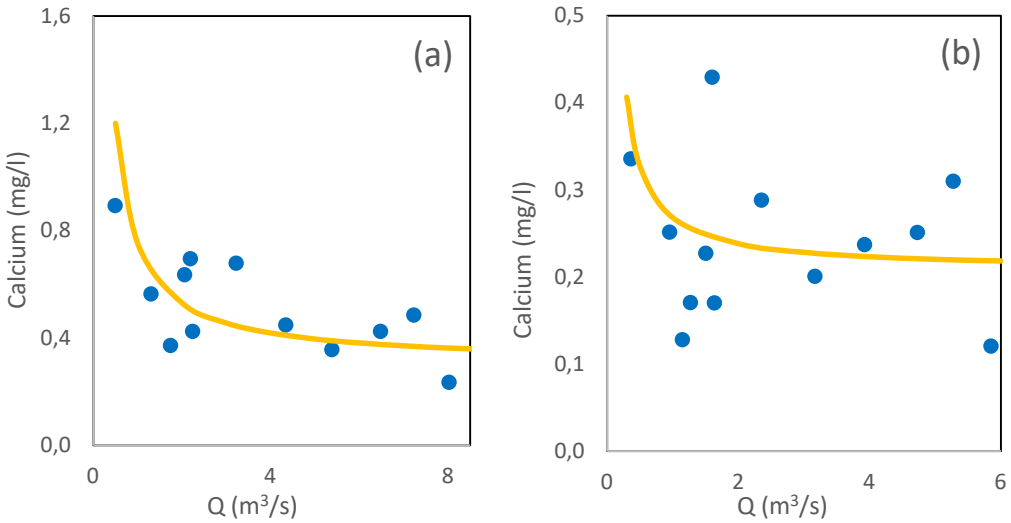

Figure 5-10 Dots represents the observed calcium concentration (mg/l) as a function of water flow (m³/s) at (a) VM Byrkjedal and (b) Hunnemonen. Yellow line represents the estimates calcium concentration (mg/l).

There was found good correlation between the observed and estimated calcium concentration (Figure 5-10, a, b). The differences were 0.01 ± 0.16 mg/l (n=12) and 0.01 ±0.09 mg/l (n=13) for VM Byrkjedal and the regulated area, respectively.

5.3.2 pH model

The regression demonstrated that the "true" pH correlated well to calcium, chloride, nitrate and colour (n=153, $F_{5,\ 148}$=101.62, R^2=0.73, p<0.05). All coefficients were individually significant (p<0.05).

$$pH \approx 5.86 + 0.87 * log(Ca^{2+}) - 0.92 * log(Cl^{-}) + 0.25 * log(NO_3^{-}) + 0.20 * log(Color)$$

Ca^{2+} mg/l, Cl^{-} mg/l, NO_3^{-} in µg/l, and color in mg Pt/l.

The formula yielded pH value close to the observed pH values (Figure 5-11). The uncertainty of the estimated pH was ±0.13.

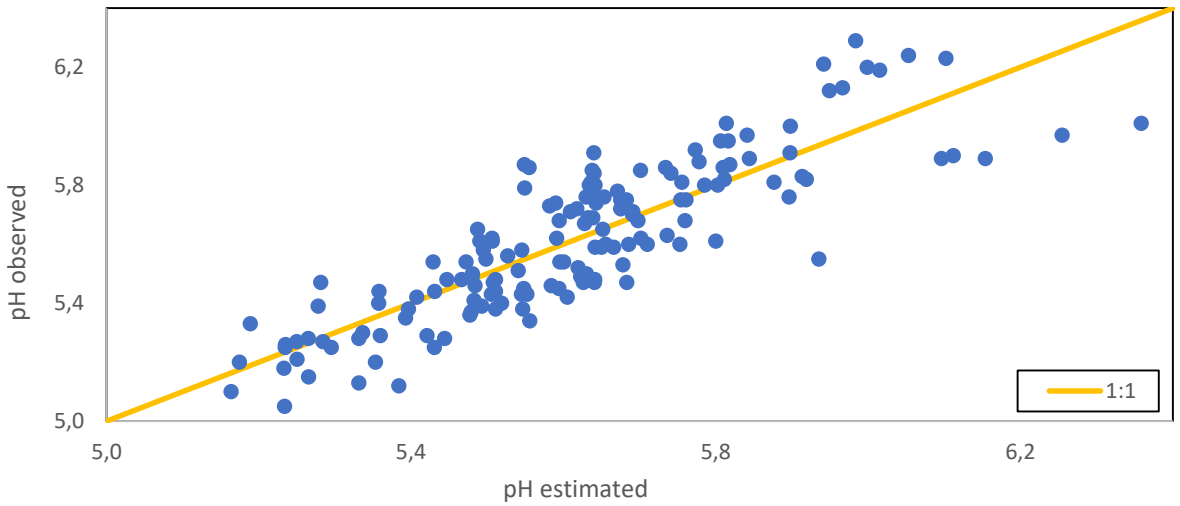

Figure 5-11 Observed pH plotted against the estimated pH.

The pH profile of the river with and without regulation was estimated at VM Byrkjedal (Figure 5-12). The same runoff estimate as in the calcium modelling was applied, 42% and 58% for the regulated area and VM Byrkjedal respectively, along with the observed parameters. The regulated river was found to have a 0.09 ±0.03 (n=12) higher pH compared to the river without the regulation (Figure 5-12).

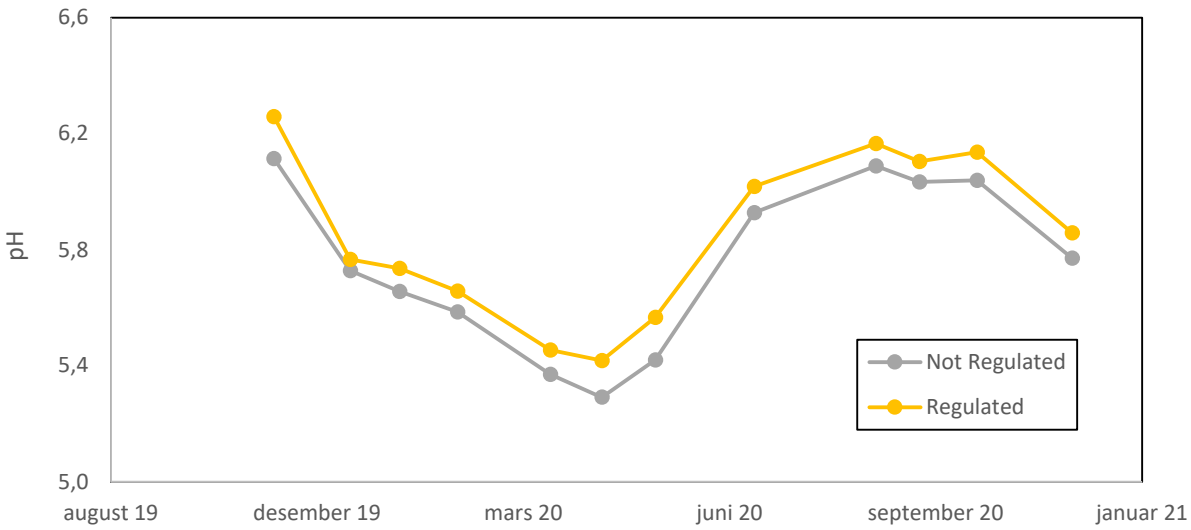

Figure 5-12 Estimated pH profiles at VM Byrkjedal, for the regulated river (yellow) and not regulated river (grey). The regulated river represents todays situation.

The annual average pH was estimated at VM Byrkjedal if the regulated area was partially opened, for 0%, 10%, 25%, 50%, 75%, and 100 % opened (Figure 5-13). Observed annual average pH at VM Byrkjedal and Hunnemonen was 5,91 and 5.57, respectively (Table 5-2).

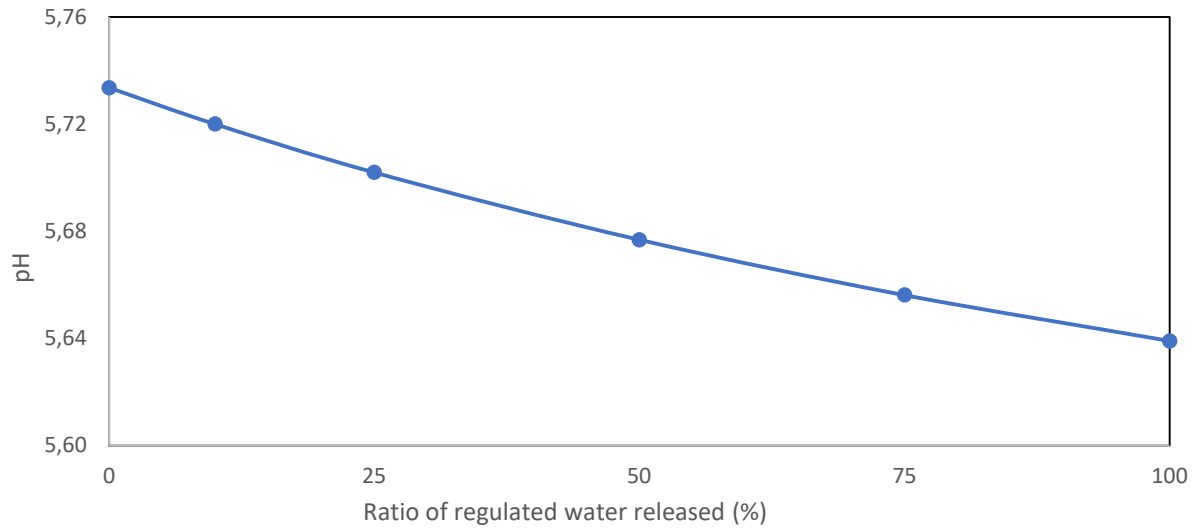

Figure 5-13 The estimated annual average pH as a function of the ratio of the regulated watershed released. 0% released is todays situation, 100% is an unregulated situation.

5.4 Other observations

5.4.1 Estimated original pH

From all the measured individual samples, 66% had a lower pH than the estimated original pH, thus 34% of the individual samples had a higher pH than the original pH (Figure 5-14). The observed pH was on average 0.07 ±0.22 (n=70) lower than the estimated original pH.

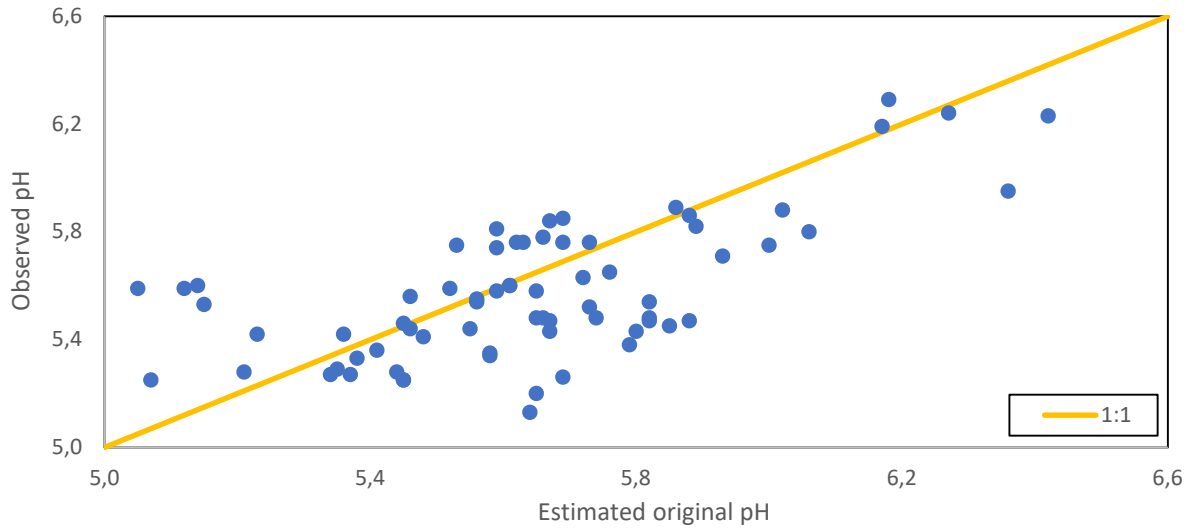

Figure 5-14 Observed pH plotted against estimated original pH for induvidual samples.

The estimated original pH profiles with the respected observed pH profiles corresponds well (Figure 5-15). The observed pH was lower than the estimated original pH from November 2019 to June 2020, for VM Byrkjedal (Figure 5-15, a). Further, the observed pH was equal compared to the estimated original pH from June 2020 to December 2020 (Figure 5-15, a). Byrkjedal, with a similar trend, observed a pH relatively lower than the estimated original pH from November 2019 to June 2020, but higher from June 2020 to November (Figure 5-15, b). In December 2020, estimated original pH and observed pH were equal (Figure 5-15, b).

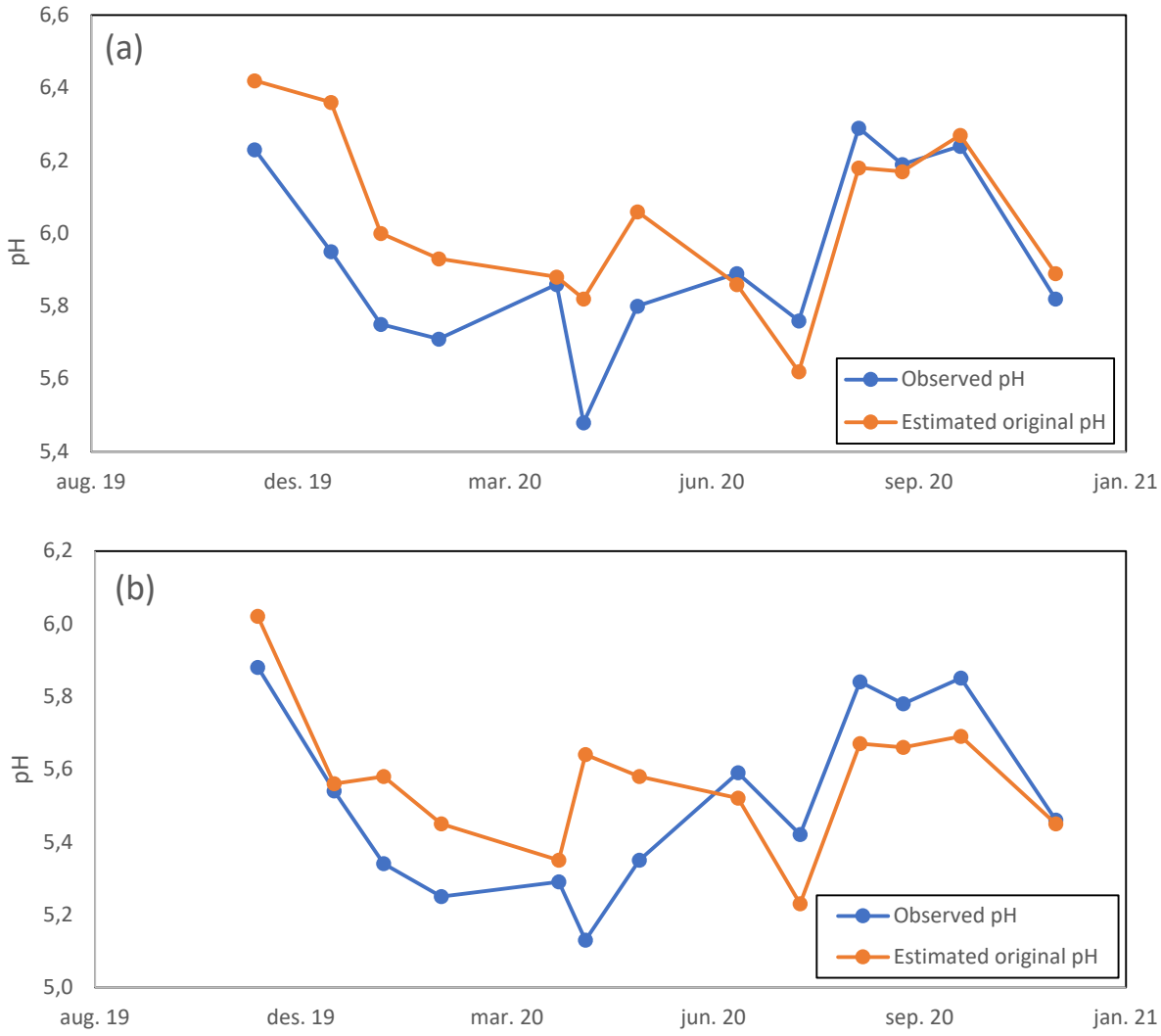

Figure 5-15 Observed and estimated original pH profiles for (a) VM Byrkjedal and (b) Byrkjedal.

5.4.2 Logging device data

Conductivity and temperature were measured by logging devices located at Hunnemonen and VM Byrkjedal (Figure 5-16). The logging device's conductivity showed no significant difference compared to the individual samples collected at Hunnemonen and VM Byrkjedal.

The conductivity increased in the late winter months, February to April, for both locations. A decreased conductivity was found in the other months, October to February and April to July.

The logging device at VM Byrkjedal was found to be above the water column from 1. November 2019 to 3. December 2019, which is why the data are excluded in the graph (Figure 5-16, a).

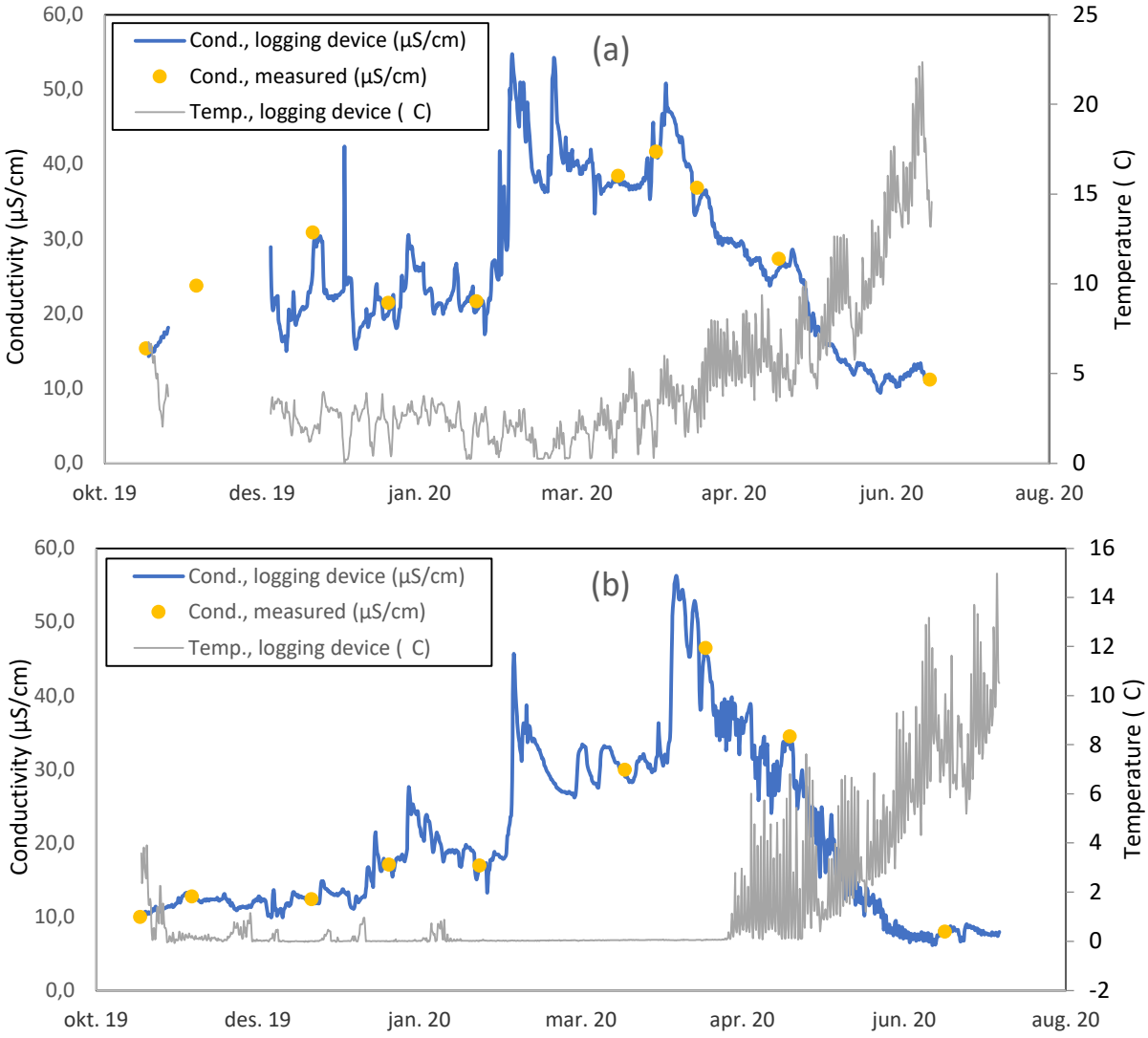

Figure 5-16 Observed conductivity (µS/cm) (Blue) with logging device with corresponding temperature (C) (Grey). Measured conductivity (µS/cm) (Yellow) from individual samples. (a) VM Byrkjedal. (b) Hunnemonen.

6 Discussion

6.1 Water chemistry

The ions of marine origin correlated well with the altitude of the sampling locations (Figure 5-3). This corresponds to literature covering dilute water bodies influenced by marine contribution in Norway (Wright & Henriksen, 1978), especially in Rogaland county, where log(chloride) was found to highly correlate with UTM-East, UTM-North and altitude (R^2=0.87, p<0.001, n=407) (Enge, 2013). The significant correlation also induces that the ion concentration of the watershed is dominated by the marine contribution. This is clarified when comparing the conductivity to calcium and chloride concentrations. A clear correlation was found between conductivity and chloride (R^2=0.98, n=156), whereas conductivity and non-marine calcium had a less significant correlation (R^2=0.43, n=156). Thus, the watershed is highly dominated by the marine deposition of ions.

The annual profile of conductivity (Figure 5-4, b, Figure 5-16, a, b) shows an increased conductivity from December 2019 to May 2020. When compared to the annual pH profile (Figure 5-4, a), the conductivity correlates negatively with the pH. The conductivity is highly dependent of the sea salt contributions, and the correlation between pH and conductivity is due the ion exchange process. Sodium from the sea salt exchange with H^+-ions in the soil of the catchment, decreasing the pH of the runoff. The same correlation was found in the pH model (5.3.2) discussed in 6.2.2., where chloride correlates significantly with pH, but negatively. Enge (2010) found a similar correlation in a pH model with conductivity, where the conductivity corelated negatively with pH.

The annual calcium profile correlates somewhat with the annual profiles of pH and conductivity (Figure 5-4), inducing some correlation with the marine contribution. Further, a significant correlation between non marine calcium flux and runoff was found (Figure 5-9). A decrease of calcium was found with increasing runoff (Figure 5-10). As the runoff increases the calcium concentration converges but increases when the runoff decreases. Thus, calcium was found to have a substantially marine and weathered origin.

Inorganic aluminum correlated with conductivity to a varying degree, where the highest altitude locations correlated better than the lower altitude locations (Figure 5-6). The correlation can be explained by the same ion exchange effect that explained the pH and

conductivity correlation. Further, the varying correlation in altitude can be explained by humic acids, measured in color, and the alkalinity. The inorganic ratio of the aluminum was found to significantly correlate with color and alkalinity, both negatively. Humic acids has the property to react with inorganic aluminum, whereas a decrease in alkalinity makes the water less resistant to acidification, and a decrease in pH increases the solubility of inorganic aluminum.

Lakes function as a mixing and accumulation body for constituents in the water. Whereas, the stratification of lakes reduces this property, and inlet water only mix in the upper layer of the lake before exiting. Stratification of the lakes was found from January 2020 to May 2020 and June 2020 to august 2020 with a period of mixing between the periods (Figure 5-8). These periods correspond with the period of increased sea salt contribution (Figure 5-16). The consequence of the stratification is that the constituents will flow faster through the watershed. Hence, the watershed will be less resistant to external impacts or changes.

6.2 Simulations

6.2.1 Calcium model

The models estimate the calcium flux as a function of observed runoff at VM Byrkjedal limnigraph (Figure 5-9, Figure 5-10). The flux was calculated from the observed calcium concentrations, with the respective observed runoff data from the date. The calcium concentration was estimated, to further be implemented in the pH model.

The model was based on regression analysis, making the variation in the estimated calcium concentration disappear. These variations were reflected in the standard deviation of the coefficient of the regression analysis. Further, no significant difference was found in the estimated calcium concentration compared to the observed.

The runoff data of the regulated area was estimated by applying the ratio between the estimated annual runoff of the fields to the observed runoff data at VM Byrkjedal limnigraph (*NVE (Noregs Vassdrags- Og Energidirektorat)*, n.d.). This estimation makes variations in runoff data of the regulated area disappear.

6.2.2 pH model

The model is a “universal” pH-model for the watershed. A total of 153 individual samples from all ten locations was used, with all depths from the two lakes (Figure 5-11). This is due

to the small sample size at every single location, with too narrow water chemistry range to make an individual pH for a specific sampling location. Hence, a deviation of estimated pH will occur and was estimated to be ±0.13.

Color, chloride, calcium, and nitrate were all individually significant ($p<0.05$) and correlated logarithmically with pH. The calcium used in the regression was non-marine calcium. Further, the calcium in the regression only explains the weathered calcium from the bedrock. Weathered calcium corelated positively with pH as expected, where weathered calcium and alkalinity were expected to be found in equivalent amount (Wright & Henriksen, 1978). The correlation between pH and sea salts were in its entirety explained through the correlation between pH and chloride, which had a negative correlation. As discussed in 6.1, an increase in deposited sea salts will give a temporarily decrease in pH. Apparently, nitrate corelated positively, which is not as expected.

The estimated pH profile of the regulated river was found to be 0.09±0.03 higher than the estimated pH profile of the river with no regulations (Figure 5-12). Hence, the regulation of the watershed gives an estimated increased pH to the field downstream the regulation.

The estimated annual average pH (Figure 5-13) of the river with different ratio of the dam opened yields a decreased pH with the increased ratio of the dam opened. For the 0% opened, the estimated annual average pH in VM Byrkjedal was 5,87. The observed annual average pH was found to be 5.91, which lies within the standard deviation of the model, ±0.13.

6.3 Original alkalinity, acidification, and original pH

The alkalinity measured was overestimated with 5% at 96.1µeq/L (Enge & Garmo, 2021). The model used to calculate original alkalinity was $1.21*[Ca]^*$ (Henriksen, 1980). The annual average estimated original alkalinity (Figure 5-7, a) for each location shows a similar pattern for all locations where around 50% of the alkalinity has been consumed., except Hunnevatn outlet where no alkalinity has been consumed. Hunnevatn outlet has a concrete dam where water is seeping out, giving it a great contact time with the dam. Relatively high calcium and alkalinity concentration was found for this location, yielding a low estimated acidification. The average estimated alkalinity for each date was found to vary. From October 2019 to June 2020 (Figure 5-7, b), around 50% of the estimated original alkalinity had been

consumed, whereas from July 2020 to December 2020 almost no estimated acidification had occurred. The same distribution over time was found when estimating the original pH.

The model used to calculate original pH, "Opprinnelig regneark.XLS" (Hindar & Wright, 2002), relies on water samples taken in the autumn (1995-2001). Simplifications in the model introduces uncertainties and inaccuracy to the estimations. Locations, sizes, or local conditions were not considered for the lakes used to establish the model. Further, the model was established with data from lakes with area from 0.06 to 1 km^2, and precipitation field from 0.7 to 20 km^2 with forest, wetlands and mountains making it representative for a wide range of waterbodies.

The estimated original pH ranged within ±0.5 of the observed pH, where the observed pH was 0.07±0.22 (n=70) lower than the estimated original pH.

The trend found in the pH profile (Figure 5-4) was found in the estimated original pH profiles (Figure 5-15), with a decreased pH from November 2019 to May 2020. This trend was expected, where the increased conductivity during that period would lower the pH, as discussed in 6.1. Further, a dilution of the buffer system during the snowmelt period would also decrease the pH (Enge, Hesthagen, et al., 2017).

6.4 Fish population

As discussed in 6.1, the watershed was found to be highly dominated by marine ions (Figure 5-5) and an increased marine contribution was found to consume alkalinity and lower the pH (Figure 5-7). Further, the marine contribution was found to highly correlate with inorganic aluminum (Figure 5-6). The inorganic ratio of aluminum also correlated well with color and alkalinity, negatively. The highest altitude area of the watershed had in general lower values of both color and alkalinity (Table 5-2).

The fish population are dependent on the marine contribution to not suffer from ion deficit (Enge & Hesthagen, 2016). At the same time the marine contribution is critical with respect to aluminum toxicity (Teien et al., 2004). Liming has been found to be a good countermeasure to the mobilization of aluminum during sea salt episodes (Teien et al., 2004). Hunnedalen watershed was found to be sensitive to changes, such as marine contribution, and the termination of liming of Lake Djupavatn could be potentially harmful for the fish population. Enge (2005) concluded that the termination of the liming of Lake

Djupavatn was justified. With the low resistance to mobilization of inorganic aluminum in the highest altitude area of the watershed, liming should still be considered.

6.5 Other anthropogenic impacts

The anthropogenic impacts, beyond the regulation, were found to be miniscule. The lake regulation, as discussed in 6.2.2, was found to increase the pH of the downstream watershed to the dam. Runoff from cabin activity and agricultural activities was found to be neglectable, where phosphate was found to be under detection limit (<3 µg/l) for all samples but one (Table 5-2). Further, no data indicated that contaminants in relation to the road gave any noticeable impact on the water quality.

7 Conclusion

The watershed was found to be highly controlled by the marine contribution of ions. A high marine contribution was found in the first half of the year. This contribution increased the conductivity, which further decreased the pH and alkalinity of the watershed. Further, the marine contribution was found to mobilize inorganic aluminum, but was limited by alkalinity and humic acids.

The human's effect on the watershed was found to be minimal with respect to contamination and nutrients input, with phosphate values below detection limit for the entire period. One exception was found below Hunnevatn outlet, where calcium, alkalinity and pH were found to be higher compared to the rest of the watershed, assumably of the great contact time with the concrete dam. The lake regulation was found to have a marginally positive effect of the water downstream the regulation.

In a watershed with low resistance to acidification, such as Hunnedalen, liming should be considered to protect the fish population. Especially in the high-altitude area where low concentration of humic acids and alkalinity were found.

9 References

Ansari, A. A., Singh Gill, S., Lanza, G. R., & Rast, W. (Eds.). (2011). *Eutrophication: Causes, consequences and control*. Springer Netherlands. https://doi.org/10.1007/978-90-481-9625-8

Berggrunn (National bedrock database). (n.d.). Retrieved October 27, 2020, from https://geo.ngu.no/kart/berggrunn_mobil/

Brezonik, P. L., & Arnold, W. (2011). *Water Chemistry: An Introduction to the Chemistry of Natural and Engineered Aquatic Systems*. Oxford University Press USA - OSO. http://ebookcentral.proquest.com/lib/uisbib/detail.action?docID=800831

Conley, D. J., Paerl, H. W., Howarth, R. W., Boesch, D. F., Seitzinger, S. P., Havens, K. E., Lancelot, C., & Likens, G. E. (2009). Controlling Eutrophication: Nitrogen and Phosphorus. *Science*, *323*(5917), 1014–1015.

Dahl, K. (1921). Undersøkelser over ørretens utdøen i det sydvestlige Norges fjeldvand. *NJFF*.

Drabløs, D., & Tollan, A. (1980). Ecological impact of acid precipitation. *SNSF Project Oslo-Ås*.

Eaton, A. D., Clesceri, L. S., & Greenberg, A. E. (Eds.). (1998). *Standard methods for the examination of water and wastewater* (20th ed.). American Public Health Association, American Water Works Association & Water Environmental Federation.

Enge, E. (2005). *Fiskeundersøkelser i Hunnedalsvassdraget 1987: Med kort oppdatert status fra 2005*.

Enge, E. (2009). *Effekter på vannkjemi, forsuringssituasjon og fiskebestander i Sira* [MSc-thesis]. University of Stavanger.

Enge, E. (2010). Modellberegninger av Vannkvalitet i Storåna: Ved ulike scenarier for slipping av minstevannføring. *Miljønotat 2-2010, Fylkesmannen i Rogaland, Miljøvernavdelingen*. https://www.fylkesmannen.no/globalassets/fm-rogaland/dokument-fmro/miljo/rapportar/undersokingar-i-kalka-vassdrag/storaana_aardal_modellberegninger_ph_2010_disht.pdf

Enge, E. (2013). Water chemistry and acidification recovery in Rogaland County. *Vann*, *01*, 78–88.

Enge, E. (2016). *Fiskeundersøkelser i Rogaland i 2015* (prosjektrapport, oppdragsgiver: Fylkesmannen i Rogaland; p. 66).

Enge, E. (2018). *Fiskeundersøkelser i Rogaland i 2017* (prosjektrapport, oppdragsgiver: Fylkesmannen i Rogaland; p. 54).

Enge, E. (2019). *Fiskeundersøkelser i Rogaland i 2018* (prosjektrapport, oppdragsgiver: Fylkesmannen i Rogaland; p. 54).

Enge, E. (2020a). *Fiskeundersøkelser i Rogaland i 2019* (prosjektrapport, oppdragsgiver: Fylkesmannen i Rogaland; p. 58).

Enge, E. (2020b). *Fiskeundersøkelser i Rogaland i 2020* (prosjektrapport, oppdragsgiver: Fylkesmannen i Rogaland; p. 45).

Enge, E., Auestad, B. H., & Hesthagen, T. (2016). Temporary Increase in Sea Salt Deposition Accelerates Recovery of Brown Trout (Salmo Trutta) Populations in Very Dilute and Acidified Mountain Lakes. *Water, Air, & Soil Pollution*, *227*(6), 208. https://doi.org/10.1007/s11270-016-2889-9

Enge, E., & Garmo, Ø. A. (2021). Estimation of low-level carbonate alkalinity from single endpoint acidimetric titration to pH=4.5. *Fundamental and Applied Limnology*, *195*(1), 1–7.

Enge, E., & Hesthagen, T. (2016). Ion deficit restricts the distribution of brown trout (Salmo trutta) in very dilute mountain lakes. *Limnologica*, *57*, 23–26.

Enge, E., Hesthagen, T., & Auestad, B. (2017). Highly dilute water chemistry during late snowmelt period affects recruitment of brown trout (Salmo trutta) in River Sira, southwestern Norway. *Limnologica*, *62*, 97–103.

Enge, E., Qvenild, T., & Hesthagen, T. (2017). Fish death in mountain lakes in southwestern Norway during late 1880s and early 1990s—A review of historical data. *Vann*, *01*, 66–80.

EPA publication SW-846. (2015). *Test Methods for Evaluating Solid Waste, Physical/Chemical Methods: Vol. Third Edition, Final Updates I (1993), II (1995), IIA (1994), IIB (1995), III (1997), IIIA (1999), IIIB (2005), IV (2008), and V (2015)*.

Gu, X., Heaney, P. J., Aarao Reis, F. D. A., & Brantley, S. L. (2020). Deep abiotic weathering of pyrite. *Science (American Association for the Advancement of Science)*, *370*(6515). https://doi.org/10.1126/science.abb8092

Henriksen, A. (1980). Acidification of freshwater: A large scale titration. *Proc. Int. Conf. Ecol. Impact Acid Precip., Norway, SNSF Project*, 68–74.

Henriksen, A. (1982). Alkalinity and Acid Precipitation Research. *VATTEN*, *38*, 83–85.

Hindar, A., & Wright, R. F. (2002). *Beregning av opprinnelig vannkjemi i forsurende innsjøer—Uttesting av en regnemodell* (LNR 4546-2002; p. 22). https://niva.brage.unit.no/niva-xmlui/bitstream/handle/11250/211742/4546_72dpi.pdf?sequence=1&isAllowed=y

Hongve, D. (1982). Kalkingsmidler til bruk i doseringsanlegg for elvekalking. *Kalkingsprosjektet, Rapport 4-82*, 32.

Huitfeldt-Kaas, H. (1922). Omaarsaken til massedød av laks og øret i Frafjordelve, Helleelven og Dirdalselven i Ryfulket høsten 1920. *Norges Jæger Og Fiskeforenings Tidsskrift*, *51*, 37–44.

Ingman, F., & Ringbom, A. (1966). Spectrophotometric determination of small amounts of magnesium and calcium employing Calmagite. *Microchemical Journal*, *10*(1), 545–553. https://doi.org/10.1016/0026-265X(66)90239-6

Jellyman, P. G., & Harding, J. S. (2014). Variable survival across low pH gradients in freshwater fish species. *Journal of Fish Biology*, *85*(5), 1746–1752. https://doi.org/10.1111/jfb.12497

Kroglund, F., & Staurnes, M. (2011). Water quality requirements of smolting Atlantic salmon (Salmo salar) in limed acid rivers. *Canadian Journal of Fisheries and Aquatic Sciences*, *56*, 2078–2086. https://doi.org/10.1139/f99-119

Ledje, U., & Jastrey, J. (2006). *Prøvefiske i kalkede vann i Rogaland 2006*. https://www.fylkesmannen.no/globalassets/fm-rogaland/dokument-fmro/miljo/rapportar/undersokingar-i-kalka-vassdrag/ambio_provefiske_i_rogaland_2006_s04cs.pdf

MET (Meteorological Institute). (n.d.). Retrieved April 1, 2021, from https://www.met.no/en

Mikhelson, K. N. (2013). *Ion-Selective Electrode* (Lecture Notes in Chemistry, Vol. 81). Springer.

Mylona, S. (1993). *Trends of Sulphur Dioxide Emissions, Air Concentrations and Depositions of Sulphur in Europe Since 1880*. Meteorological Synthesizing Centre-West, Norwegian Meteorological Institute.

Norton, S. A., & Henriksen, A. (1983). The importance of CO2 in evaluation of effects of acidic deposition. *VATTEN*, *39*, 346–353.

NVE (Noregs Vassdrags- og energidirektorat). (n.d.). Retrieved May 15, 2021, from https://www.nve.no/

Raikos, N., Fytianos, K., Samara, C., & Samanidou, V. (1988). Comparative study of different techniques for nitrate determination in environmental water samples. *Fresenius' Zeitschrift Für Analytische Chemie*, *331*(5), 495–498. https://doi.org/10.1007/BF00467037

Samdal, J. E. (1987). Noen resultater fra NIVA's forskning innen sur nedbør. *Vann*, *3*.

Schoepp, W., Posch, M., Mylona, S., & Johansson, M. (2003). Long-term development of acid deposition (1880-2030) in sensitive freshwater regions in Europe. *Hydrology and Earth System Sciences - HYDROL EARTH SYST SCI*, *7*, 436–446. https://doi.org/10.5194/hess-7-436-2003

Snekvik, E. (1974). Sure innsjøer og fiskebestand i Rogaland, Vest-Agder, Aust-Agder, Telemark. Sammenstilling av opplysninger innhentet hos innlandsfiskenemdene i de fire fylkene. *Direktoratet for Vilt Og Ferskvannsfisk, Fiskeforskningen*, *2*, 50.

Snoeyink, V. L., & Jenkins, D. (1980). *Water chemistry* (p. XIII, 463). Wiley.

Statistisk sentralbyrå (Statistics Norway). (n.d.). Retrieved May 15, 2021, from https://www.ssb.no/

Stølen, C. (2019). *Effects of Rockfill Dams and Rock Dumps on Downstream Water Chemistry* [University of Stavanger]. http://hdl.handle.net/11250/2644545

Stumm, W., & Morgan, J. J. (1995). *Aquatic Chemistry: Chemical Equilibria and Rates in Natural Waters* (3rd ed., Vol. 126). John Wiley & Sons, Incorporated. http://ebookcentral.proquest.com/lib/uisbib/detail.action?docID=1550541

Teien, H.-C., Salbu, B., Heier, L., Kroglund, F., & Rosseland, B. O. (2005). Fish mortality during sea salt episodes—Catchment liming as a countermeasure. *Journal of Environmental Monitoring : JEM*, *7*, 989–998. https://doi.org/10.1039/b507086d

Teien, H.-C., Standring, W., Salbu, B., Marskar, M., Kroglund, F., & Hindar, A. (2004). Mobilization of aluminium and deposition on fish gills during sea salt episodes—Catchment liming as countermeasure. *Journal of Environmental Monitoring : JEM*, *6*, 191–200. https://doi.org/10.1039/b314708h

Wright, R. F., & Henriksen, A. (1978). Chemistry of small Norwegian lakes, with special reference to acid precipitation 1: Chemistry of Norwegian lakes. *Limnology and Oceanography*, *23*(3), 487–498. https://doi.org/10.4319/lo.1978.23.3.0487

Appendix A: PREELIMINARY MANUS - Case study: Use of a nitrate ion selective electrode in unpolluted oligotrophic water

Espen Enge (ass. professor, UiS)
Mats G. Grendal (MSc-student, UiS)

ABSTRACT

Due to numerous possible interferences, ISE (Ion Selective Electrode) is normally considered a highly unreliable method for determining nitrate in natural waters. However, due to the simplicity, the low detection limit, and the modest costs, it is of interest to test if ISE is applicable at least in some types of water. Our study confirmed previous research, demonstrating that ISE measurements, even when applied on unpolluted water samples, overestimated the nitrate concentrations. However, when considering the interfering ions, an accuracy of ±55 µg/l in the range 20-570 µg N/l was achieved. We conclude that the ISE-method, with an adjustment for interferences, may be used for screening purposes, but lack the accuracy required for high-precision work. We suggest that these findings are valid for other brands of electrodes too.

INTRODUCTION

Currently, photometry and ion chromatography (IC) are among the most popular methods for determining nitrate in water samples. If low concentrations (<1 mg/l) are to be measured, the first method normally requires a reduction step, followed by determining the nitrate as nitrite, while the latter method (IC) includes extensive instrumentation. Therefore, there is a scarcity of simple methods for determining low-level nitrate.

ISE's (Ion Selective Electrodes) are available for numerous ions, including nitrate. Electrodes are relatively cheap, typical NKr. 5000-15000, and require only a pH-meter with mV readability and a magnetic stirrer; the latter two being standard laboratory equipment.

A general problem with ISE's is that they, despite the name, are never 100% selective. H^+- and F^--electrodes have limited susceptibility to interferences, but they are rare exceptions (Mikhelson 2013). Furthermore, Rike-Hansen and Rødne (2016) demonstrated excellent accuracy and precision of the Ca-electrode in natural waters from southwestern Norway. The nitrate electrode, on the other hand, is susceptible to numerous interfering ions and it is considered a highly unreliable method for determining nitrate in natural water (Raikos et al. 1988). In a more recent study, Ims (2019) found serious deviations between nitrate measured by the electrode ISE25NO3 and colorimetric determinations ("Merck Sectroquant") when analysing water from the polluted brook "Leikvollbekken" in Stavanger. Moreover, typical interferences for the nitrate electrode are normal occurring components of water as bicarbonate, chloride, and organic anions.

Due to the simplicity, the low detection limit, and the modest cost, it is of interest to test if ISE is applicable at least in some types of water. Here, we test the Radiometer ISE25NO3 electrode on water samples from unpolluted lakes and brooks from south western Norway.

MATERIAL AND METHODS

This study applies an empirical approach. We statistically compare ISE and colorimetric determination and try to explain the discrepancies by potential interferences.

Sampling sites

Samples were collected in December 2020 in nine pristine, oligotrophic lakes and brooks, located at 120-650 m a.s.l. In the sampling area, the alkalinity of the waters is generally low and has moderate levels of organic matter ("color"). Determinations of pH, conductivity, "color", alkalinity, chloride, nitrate (ISE) and nitrate (colorimetric) were performed at all samples. By mixing these nine samples in different ratios, including spiking a number of them with Na_2SO_4, KNO_3, $NaHCO_3$, and seawater to extend the concentration ranges, we made 35 additional samples.

Because all parameters included in the statistical analyses (see below) were conservative, we, with one exception, calculated the concentrations of the mixed samples simply by using the analyses of the original samples and mixing ratio. For conductivity, we measured the conductivity for all mixed samples.

Table 1. Concentration ranges for the applied parameters.

Parameter	Range	Unit
Chloride	1.2 – 16.8	mg/l
Alkalinity	<0 – 129	µeq/l
Conductivity	7 – 72	µS/cm
Color	4 – 70	mg Pt/l
Nitrate (colorimetric)	21 - 571	µg N/l

Determinations of Nitrate

Colorimetric determination ("reference"): The determination was modified after "Standard Methods" 4500-NO_3-E Cadmium Reduction Method (Eaton et al. 1995). This method includes the use of highly toxic cadmium as a reducing agent. Due to safety precautions, we modified the method and used Zn-powder as a reductor. Zinc is also an acknowledged reducing agent for nitrate (e.g. Merino, 2009). The standard solution (1000 mg/l NO_3-N) was made of KNO_3 (Merck, p.a. quality). To account for possible interferences we applied the standard addition technique. Additional to the direct measurements, samples +100 µg/l and +200 µg/l were measured. Absorption was determined at 550 nm in 40 mm glass cells using a Shimadzu spectrophotometer UV-120-01. *ISE-determination:* Nitrate was measured at all the 44 samples with polymer membrane ion-selective electrode Radiometer ISE25NO3,

equipped with the recommended reference electrode Radiometer REF201. $(NH_4)_2SO_4$ 1M was used as ISA (addition: 1 ml/10 ml of sample). To assure nitrate concentrations beyond the detection limit (70 µg/l) and within the linear range of the electrode, 950 µg/L NO_3-N was added to every sample. The inner solution following the electrode (S41M004) was diluted 1:10, due to relatively low concentrations of nitrate (c.f. Mikhelson, 2013).

Other determinations

Alkalinity: Alkalinity was determined by titrating the sample to fixed endpoint pH=4.50 with 0.0025 N H_2SO_4. Alkalinity ("ALK_E") was calculated according to Henriksen (1982). *Conductivity:* Conductivity was determined according to "Standard Methods" 2510 (Eaton et al., 1995), using an Amber Science conductivity meter (mod. 1056). *Color:* Color was determined according to former "Norwegian Standard" NS 4722. The samples were measured unfiltered at 445 nm in 40 mm glass cells with a Shimadzu spectrophotometer UV-20-01. *Chloride:* Chloride was measured potentiometric using124 Radiometer ISE/HS25Cl electrode. A VWR double junction electrode with 0.1 M KNO_3 in the outer chamber was used as a reference electrode. ISA (1 M KNO_3 in 0.005 M HNO_3) was added to all samples (1 ml/10 ml of sample).

Statistics

Multiple regression was applied on nitrate (colorimetric) v.s. nitrate ISE, chloride, color, alkalinity, and conductivity.

RESULTS

The regression demonstrated that "true" nitrate was highly correlated to nitrate (ISE), color, alkalinity, conductivity and chloride (r^2=0.964, $F_{5,38}$=204.10, p<0.001, n=44). All the regression coefficients were individually significant (p<0.001):

$$\boldsymbol{NO_3 \approx 0.84 \quad NO_3(ISE) \quad 2.0 \quad Color \quad 2.7 \quad ALK_E + 7.4 \quad Cond \quad 28 \quad Cl \quad 11}$$

The regression formula yielded nitrate values close to the observed values (fig. 1b), while the uncorrected values were associated with serious overestimation of the nitrate concentrations (fig. 1a). Uncertainty of the estimated ("adjusted") nitrate values was ±55 µg/l.

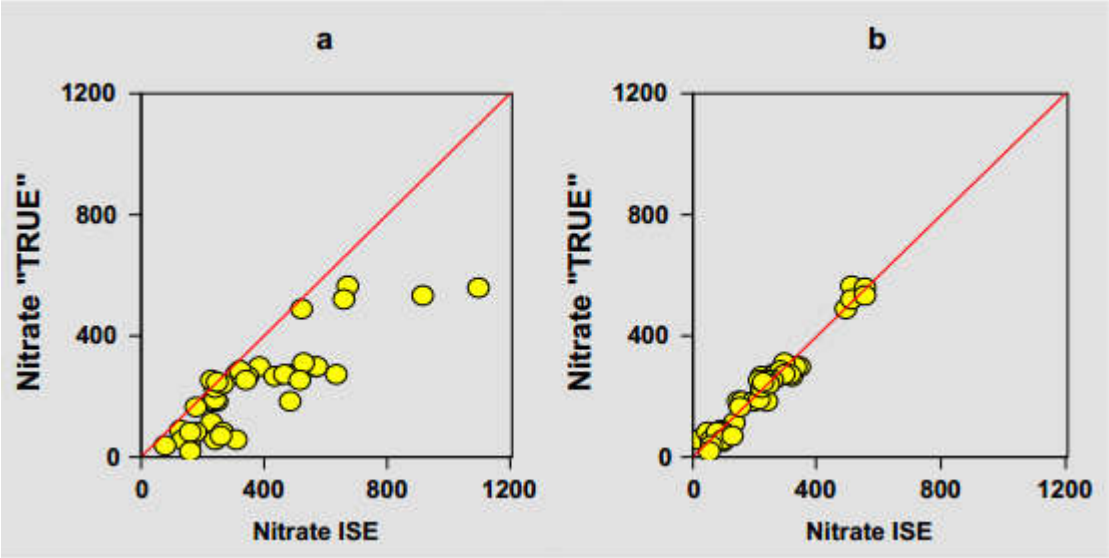

Fig.1: "True" nitrate values (colorimetric determination) vs. measured values using ISE (a) and ISE-values adjusted using the regression formula.

The Nernst-slopes of the calibration curves were only ≈80%, indicating that the measurements, despite the addition of 950 µg/l nitrate, were performed below the linear range of the calibration curve.

DISCUSSION

There is a scarcity of simple methods for determining low-level nitrate. The colorimetric methods comprising a nitrate reduction step are either very labor-intensive or require expensive automated analyzers. IC is an alternative method but requires also expensive instrumentation.

Here, we demonstrated that the ISE-determinations, even when performed in unpolluted pristine oligotrophic water, were associated with severe overestimation of the nitrate concentrations. However, when considering important electrode interferences, we established an acceptable empiric relationship between "true" nitrate and ISE-nitrate.

To some extent, most anions interfere positively in nitrate ISE-measurements, while no effects of cations are listed. In the correction formula, color (representing organic anions), alkalinity (bicarbonate), and chloride contributed negatively. This is consistent with an expected nitrate overestimation due to these ions, which have to be subtracted.

The observed positive contribution from conductivity was not expected. However, four samples from Lake Vikastølsvatn were included in our data set. From this lake, "full" analyses from other samples exist (E. Enge and H. v.d. Hoeven, unpublished data). Multiple regression revealed that sulfate was positively correlated (r^2=0.58, n=32) to conductivity ($p<0.001$) and negatively correlated to alkalinity ($p<0.01$), nitrate ($p<0.01$), and Cl ($p<0.001$). These are the same variables and with the same signs as in the nitrate correction formula. Therefore, these combinations, including conductivity with a positive sign, were most likely an indirect

representation of sulfate. Sulfate is a minor interfering ion in ISE nitrate determinations (Mikhenson 2013).

We calibrated the electrode in the range 50-800 µg/l which, including the initial addition of 0.95 mg/l (see "Methods"), represented nitrate concentrations between 1000 and 2000 µg N/l. This was expected to be close to the linear range of the calibration curve for the ISE25NO3 (c.f. user manual). With a slope of 80%, this was apparently not in the linear range. According to EPA (2015), nitrate electrodes, in general, has a linear range of typical 5-200 mg/l and stated that that nitrate concentrations below this limit will be biased high. Therefore, we cannot reject the possibility that direct or indirect effects of measuring in the non-linear segment of the calibration curve may account for some of the discrepancies between the ISE- and colorimetric measurements.

While accredited analyses are required for documentation purposes for e.g. waterworks, breweries, food industries (etc.), internal control does normally not require the utmost accuracy and precision. Moreover, environmental consultants, educational institutions, or other businesses or organizations with too limited number of samples to justify investments in expensive equipment, may also find nitrate electrodes useful. By adjusting for interferences an accuracy of ±55 µg/l was achieved, probably acceptable for the listed purposes.

An important question is if our findings apply to other brands of electrodes. This issue has lately become highly relevant because Hach Company recently has discontinued the Radiometer ISE25NO3-electrode. However, available specifications from other brands of nitrate electrodes show primarily the same interferences and with the same ranking of severity. Moreover, the selectivity of typical ion-exchange-based anion electrodes, in general, depends on the affinity of polar anions to a lipophilic electrode membrane (Mikhelson 2013), which follows the "Hofmeister series" (Hofmeister 1888). Therefore, these limitations are general issues, not associated with a specific brand of electrodes. This suggests that our results most likely are valid for other electrodes too. However, we cannot reject a possible need for "recalibrating" the correction formula if other electrodes are to be used.

REFERENCES

Eaton, A.D., Clesceri, L.S., Greenberg, A.E. (eds), 1995. Standard methods for the examination of water and wastewater (19. edition). *American Public Health Association, American Water Works Association & Water Environment Federation, Washington DC.*

EPA 2007: SW-846 Test Method 9210A: Potentiometric Determination of Nitrate in Aqueous Samples with an Ion-Selective Electrode. *United States Environmental Protection Agency.*

Hofmeister, F. 1888. Zur Lehre von der Wirkung der Salze. *Arch. Exp. Pathol. Pharmacol. 24 (4–5): 247–260.*

Ims, K. 2019. Nitrogen retention in mature constructed wetlands. *MSc-thesis, University of Stavanger.*

Merino, L. 2009. Development and validation of a method for determination of residual nitrite/nitrate in foodstuffs and water after zinc reduction. *Food Analytical Methods, 2(3), 212-220.*

Mikhelson, K.N. 2013. Ion-Selective Electrodes. *Springer-Verlag, Berlin.*

Raikos, N., Fytianos, K., Samara, C., and Samanidou, V. 1988. Comparative study of different techniques for nitrate determination in environmental water samples. *Fresenius' Zeitschrift für analytische Chemie, 331(5), 495-498.*

Rike-Hansen, H.E. and Rødne, C.S. 2016. Sammenligning av ioneselektiv elektrode og atomabsorpsjonsspektroskopi til måling av kalsium i naturlig vann. (Comparison of Ion Selective Electrode and Atomic Absorption Spectroscopy for Measurement of Calcium in Natural Water). *BSc-thesis, University of Stavanger.*

Appendix B: Water analysis

All measured data.

Location	Date	Temp. (C)	pH	Conductivity (µS/cm)	Color (mg Pt/l)	ALKe (µeq/l)	K (mg/l)	Ca (mg/l)	Cl (mg/l)	Na (mg/l)	Mg (mg/l)	Diss-P (µg/l)	Tot-P (µg/l)	Al (µg/l)	LAl (µg/l)	SO_4 (mg/l)	NO_3 (µg/l)
Vm byrkjedal	25.10.2019		5,83	15,4	24	13	0,03	0,39	2,5	1,7	0,21			49	8	1,30	
Hunnemo	25.10.2019		5,47	10	13	2		0,16	1,5	1,0				43	15		
Gilja	10.11.2019		6,2	24,9	11	30	0,17	0,84	4,3	2,9		<3		24	4		321
Byrkjedal	10.11.2019		5,88	18,9	20	18	0,05	0,51	3,5	2,3	0,26	<3		35	9	1,47	86
VM byrkjedal	10.11.2019		6,23	23,8	8	34	0,11	0,97	3,7	2,6	0,28	<3		19	6	1,64	363
Øvstabø brook	10.11.2019		5,55	12,4	9	6	0,07	0,59	2,8	1,9		<3		26	10		138
Øvstabø river	10.11.2019		5,91	16,8	11	20	0,05	0,26	2,1	1,4		<3		26	7		70
Djupvatn brook	10.11.2019		5,72	12,4	19	9	0,05	0,31	2,2	1,4		<3		37	12		23
Hunnevatn outlet	10.11.2019		5,8	13,8	17	25	0,08	0,50	2,3	1,4		<3		43	19		19
Hunnemo	10.11.2019		5,81	12,8	3	17	0,05	0,38	1,9	1,4		<3		20	11		87
Gilja	17.12.2019		5,95	27,3	14	17	0,18	0,71	5,5	3,2		<3		29	7		256
Byrkjedal	17.12.2019		5,54	18,3	23	5	0,11	0,32	3,5	2,1	0,27	<3		39	8	1,27	109
VM byrkjedal	17.12.2019		5,95	30,9	11	17	0,21	0,76	5,8	3,8	0,39	<3		27	6	1,33	322
Øvstabø brook	17.12.2019		5,43	12,8	13	3	0,12	0,19	2,4	1,4		<3		36	11		134
Øvstabø river	17.12.2019		5,68	15,8	15	8	0,08	0,38	3,0	1,8		<3		33	12		155
Djupvatn brook	17.12.2019		5,68	11,9	20	10	0,07	0,25	2,1	1,3		<3		39	11		86
Hunnevatn outlet	17.12.2019		5,9	15	13	40	0,11	0,67	2,1	1,4		<3		36	11		109
Hunnemo	17.12.2019		5,7	12,4	6	11	0,09	0,27	2,0	1,3		<3		34	16		117

Location	Date	Temp. (C)	pH	Conductivity (µS/cm)	Color (mg Pt/l)	ALKe (µeq/l)	K (mg/l)	Ca (mg/l)	Cl (mg/l)	Na (mg/l)	Mg (mg/l)	Diss-P (µg/l)	Tot-P (µg/l)	Al (µg/l)	LAl (µg/l)	SO_4 (mg/l)	NO_3 (µg/l)
Gilja	10.01.2020		5,75	22,7	12	14	0,16	0,57	4,5	2,7		<3		38	12		198
Byrkjedal	10.01.2020		5,34	18,8	18	4	0,10	0,31	3,6	2,2	0,26	<3		44	13	1,10	114
VM byrkjedal	10.01.2020		5,75	21,5	10	13	0,15	0,54	4,2	2,5	0,28	<3		32	9	1,27	211
Øvstabø brook	10.01.2020		5,3	16,4	10	2	0,10	0,19	3,1	1,8		<3		38	13		115
Øvstabø river	10.01.2020		5,45	17,8	14	6	0,11	0,33	3,5	2,1		<3		38	13		131
Djupvatn brook	10.01.2020		5,5	13,2	19	8	0,09	0,23	2,3	1,5		<3		41	11		105
Hunnevatn outlet	10.01.2020		5,89	16,6	9	43	0,15	0,74	2,5	1,7		<3		34	-2		177
Hunnemo	10.01.2020		5,37	17,1	7	4	0,12	0,27	3,3	1,9		<3		45	16		142
Lake Hunnevatn 0m	10.01.2020	4	5,38	15,6	12	5		0,24	2,6	1,7	0,22			44	21		119
Lake Hunnevatn 5m	10.01.2020	4	5,4	13,2	12	4		0,18	2,2	1,4	0,19			39	14		110
Lake Hunnevatn 10m	10.01.2020	5	5,49	12,1	14	6		0,20	1,9	1,3	0,20			35	10		98
Lake Hunnevatn 20m	10.01.2020	5	5,61	11,9	13	10		0,29	1,8	1,3	0,19			39	14		98
Gilja	07.02.2020		5,72	22,7	12	10	0,20	0,53	4,6	2,7		<3	<3	41	16		143
Byrkjedal	07.02.2020		5,25	20,4	16	0	0,14	0,31	4,1	2,4	0,27	<3	3,1	46	19	1,05	77
VM byrkjedal	07.02.2020		5,71	21,7	12	10	0,17	0,52	4,5	2,7	0,29	<3	<3	37	12	1,10	156
Øvstabø brook	07.02.2020		5,18	22,5	8	-1	0,16	0,26	4,7	2,6		<3	<3	42	23		104
Øvstabø river	07.02.2020		5,47	20,4	14	12	0,18	0,37	4,3	2,5		<3	<3	38	14		95
Djupvatn brook	07.02.2020		5,39	18,2	17	5	0,15	0,30	3,6	2,1		<3	<3	42	21		84
Hunnevatn outlet	07.02.2020		5,83	19,6	8	34	0,19	0,69	3,5	2,1		<3	<3	40	16		187
Hunnemo	07.02.2020		5,38	17	7	8	0,17	0,32	3,4	1,9		<3	<3	55	31		96
Lake Djupavatn 0m	07.02.2020	2	5,36	18	17	5	0,11	0,30	3,7	2,1	0,27	<3	<3	41	15	0,99	72
Lake Djupavatn 5m	07.02.2020	3	5,63	12,3	20	12	0,10	0,28	2,2	1,4	0,19	<3	<3	40	12	0,92	90
Lake Djupavatn 10m	07.02.2020	4	5,6	13,1	19	12	0,09	0,28	2,3	1,5	0,17	<3	<3	38	11	0,95	94
Lake Djupavatn 20m	07.02.2020	4	5,6	12,4	20	13	0,07	0,30	2,2	1,4	0,18	<3	<3	38	11	0,94	87

Location	Date	Temp. (C)	pH	Conductivity (µS/cm)	Color (mg Pt/l)	ALKe (µeq/l)	K (mg/l)	Ca (mg/l)	Cl (mg/l)	Na (mg/l)	Mg (mg/l)	Diss-P (µg/l)	Tot-P (µg/l)	Al (µg/l)	LAl (µg/l)	SO_4 (mg/l)	NO_3 (µg/l)
Gilja	23.03.2020		5,74	36,9	8	11	0,49	0,82	8,5	4,5				36	13		207
Byrkjedal	23.03.2020		5,2	32,8	12	-2		0,48	7,6	3,9	0,50			58	28		125
VM byrkjedal	23.03.2020		5,87	38,5	6	11		0,89	9,2	4,7	0,59			31	11	1,79	176
Øvstabø brook	23.03.2020		5,21	28,7	8	-2	0,31	0,36	6,6	3,4				55	28		139
Øvstabø river	23.03.2020		5,5	34,5	9	6	0,37	0,66	8,2	4,2				44	19		158
Djupvatn brook	23.03.2020		5,46	20,8	15	6	0,34	0,37	4,6	2,4				42	13		103
Hunnevatn outlet	23.03.2020		5,86	29	6	37	0,44	0,89	6,1	3,3				44	20		164
Hunnemo	23.03.2020		5,28	30	5	6	0,42	0,58	6,9	3,4				64	44		144
Lake Hunnevatn 0m	23.03.2020	0,2	5,25	27	9	1	0,25	0,34	5,9	3,1	0,38		<3	53	30	1,02	152
Lake Hunnevatn 5m	23.03.2020	0,3	5,28	24,8	9	2	0,27	0,33	5,5	2,9	0,37		<3	51	25	1,04	170
Lake Hunnevatn 10m	23.03.2020	0,6	5,43	15,6	11	7	0,28	0,27	3,1	1,7	0,22		<3	48	19	0,98	138
Lake Hunnevatn 20m	23.03.2020	1,5	5,47	14	12	10	0,32	0,27	2,6	1,5	0,22		<3	43	15	0,91	130
Byrkjedal, blank	04.04.2020		5,29	32,6	10	2	0,24	0,54	7,4	3,8	0,53		<3	56	27	1,51	134
VM byrkjedal	04.04.2020		5,86	41,7	6	13	0,33	0,94	9,8	5,2	0,63		<3	30	9	1,58	214
Lake Djupavatn 0m	04.04.2020	0,4	5,41	19,6	14	6	0,20	0,35	4,1	2,2	0,31		<3	48	19	1,24	75
Lake Djupavatn 5m	04.04.2020	0,9	5,52	14,7	17	10	0,20	0,30	2,8	1,6	0,25		<3	45	14	1,11	78
Lake Djupavatn 10m	04.04.2020	1	5,48	15,7	19	8	0,23	0,32	2,9	1,7	0,25		<3	44	12	1,10	82
Lake Djupavatn 20m	04.04.2020	1,6	5,47	15,8	23	13	0,37	0,33	2,8	1,7	0,22		<3	44	14	1,10	67

Location	Date	Temp. (C)	pH	Conductivity (µS/cm)	Color (mg Pt/l)	ALKe (µeq/l)	K (mg/l)	Ca (mg/l)	Cl (mg/l)	Na (mg/l)	Mg (mg/l)	Diss-P (µg/l)	Tot-P (µg/l)	Al (µg/l)	LAl (µg/l)	SO_4 (mg/l)	NO_3 (µg/l)
Gilja	17.04.2020		5,51	35,4	12	11	0,29	0,67	7,7	4,4				54	27		148
Byrkjedal	17.04.2020		5,13	34	15	-2	0,28	0,45	7,4	4,2	0,48		<3	61	41	1,30	101
VM byrkjedal	17.04.2020		5,48	36,9	11	7	0,33	0,66	8,0	4,5	0,44		<3	53	25	1,51	165
Øvstabø brook	17.04.2020		5,1	38,4	9	-2	0,30	0,40	8,6	4,8				83	61		163
Øvstabø river	17.04.2020		5,29	38,6	13	3	0,27	0,53	8,8	4,9				56	31		163
Djupvatn brook	17.04.2020		5,44	23,4	17	5	0,22	0,35	4,9	2,8				38	17		102
Hunnevatn outlet	17.04.2020		5,75	36	8	33	0,33	0,90	7,5	4,3				60	38		192
Hunnemo	17.04.2020		5,05	46,5	8	-2	0,30	0,53	10,4	5,7				105	86		208
Lake Hunnevatn 0m	17.04.2020	0,4	5,2	35,9	11	1	0,20	0,38	7,9	4,4	0,59		<3	62	39	1,36	119
Lake Hunnevatn 5m	17.04.2020	0,5	5,26	30,6	11	4	0,18	0,36	6,6	3,7	0,51		<3	60	38	1,18	106
Lake Hunnevatn 10m	17.04.2020	0,7	5,38	19,5	11	6	0,18	0,29	3,8	2,2	0,34		<3	48	25	0,96	72
Lake Hunnevatn 20m	17.04.2020	1,3	5,45	16	13	10	0,19	0,30	2,9	1,7	0,28		<3	40	18	0,97	57

Location	Date	Temp. (C)	pH	Conductivity (µS/cm)	Color (mg Pt/l)	ALKe (µeq/l)	K (mg/l)	Ca (mg/l)	Cl (mg/l)	Na (mg/l)	Mg (mg/l)	Diss-P (µg/l)	Tot-P (µg/l)	Al (µg/l)	LAl (µg/l)	SO_4 (mg/l)	NO_3 (µg/l)
Gilja	13.05.2020		5,79	27,8	11	12	0,25	0,56	5,9	3,4				27	10		117
Byrkjedal	13.05.2020		5,35	24,8	15	0	0,20	0,36	5,2	3,0	0,33		<3	39	16	1,39	97
VM byrkjedal	13.05.2020		5,8	27,4	10	9	0,22	0,68	5,9	3,4	0,39		<3	30	11	1,56	108
Øvstabø brook	13.05.2020		5,12	32,4	10	-4	0,23	0,47	6,9	3,9				65	39		134
Øvstabø river	13.05.2020		5,4	28,6	14	3	0,34	0,40	6,2	3,5				44	20		99
Djupvatn brook	13.05.2020		5,39	26,7	17	3	0,24	0,32	5,8	3,3				43	19		93
Hunnevatn outlet	13.05.2020		5,84	28,7	5	37	0,24	0,89	5,6	3,2				39	19		129
Hunnemo	13.05.2020		5,15	34,5	5	-1	0,24	0,45	7,6	4,1				97	77		160
Lake Hunnevatn 0m	13.05.2020	0,8	5,25	26,1	10	2	0,23	0,30	5,5	3,1	0,38		<3	58	37	1,13	103
Lake Hunnevatn 5m	13.05.2020	1,1	5,28	26	11	2	0,20	0,30	5,4	3,0	0,38		<3	56	32	1,15	112
Lake Hunnevatn 10m	13.05.2020	1,2	5,27	26,6	10	2	0,19	0,31	5,7	3,1	0,39		<3	64	39	1,22	120
Lake Hunnevatn 20m	13.05.2020	1,7	5,27	26,9	10	2	0,15	0,33	5,6	3,1	0,38		<3	61	44	1,21	113
Lake Djupavatn 0m	13.05.2020	0,3	5,33	24,7	16	4	0,16	0,26	5,2	3,0	0,35		<3	33	9	1,22	75
Lake Djupavatn 5m	13.05.2020	1	5,42	19,9	18	7	0,11	0,29	4,0	2,3	0,27		<3	41	17	1,15	71
Lake Djupavatn 10m	13.05.2020	1,3	5,44	17,2	19	8	0,09	0,29	3,3	1,9	0,24		<3	39	19	1,06	67
Lake Djupavatn 20m	13.05.2020	1,9	5,47	15,9	18	10	0,09	0,31	2,8	1,7	0,21		<3	36	17	1,03	74

Location	Date	Temp. (C)	pH	Conductivity (µS/cm)	Color (mg Pt/l)	ALKe (µeq/l)	K (mg/l)	Ca (mg/l)	Cl (mg/l)	Na (mg/l)	Mg (mg/l)	Diss-P (µg/l)	Tot-P (µg/l)	Al (µg/l)	LAl (µg/l)	SO_4 (mg/l)	NO_3 (µg/l)
Gilja	30.06.2020		6	12,8	22	16	0,30	0,36	2,2	1,6				29	9		136
Byrkjedal	30.06.2020		5,59	17,5	40	10	0,13	0,35	3,4	2,2	0,25		<3	52	7	1,54	58
VM byrkjedal	30.06.2020		5,89	11,2	27	14	0,16	0,28	1,8	1,4	0,16		<3	40	4	1,27	96
Øvstabø brook	30.06.2020		5,54	11,1	12	5	0,17	0,15	1,7	1,1				23	7		54
Øvstabø river	30.06.2020		5,65	9,2	24	9	0,20	0,19	1,5	1,1				36	9		35
Djupvatn brook	30.06.2020		5,69	13,3	21	9	0,24	0,29	2,5	1,6				35	5		51
Hunnevatn outlet	30.06.2020		5,89	12,5	14	34	0,27	0,60	1,8	1,3				42	9		121
Hunnemo	30.06.2020		5,49	8	13	5	0,22	0,15	1,3	0,9				35	8		16
Lake Djupavatn 0m	30.06.2020	14,3	5,65	13,1	15	9	0,19	0,24	2,5	1,5	0,20		<3	34	9	0,85	38
Lake Djupavatn 5m	30.06.2020	10,1	5,55	14,6	18	9	0,13	0,28	2,9	1,7	0,21		<3	41	11	0,89	39
Lake Djupavatn 10m	30.06.2020	5	5,48	15,6	18	10	0,23	0,28	3,0	1,8	0,22		<3	35	10	0,95	33
Lake Djupavatn 20m	30.06.2020	5	5,48	15,7	18	10	0,22	0,28	3,1	1,8	0,22		<3	39	12	0,88	32
Gilja	30.07.2020		5,82	11,6	34	13	0,21	0,31	1,9	1,5				52	10		104
Byrkjedal	30.07.2020		5,42	14,5	52	6	0,12	0,23	2,5	1,9	0,16		<3	61	7	1,43	57
VM byrkjedal	30.07.2020		5,76	10	35	12	0,15	0,23	1,5	1,3	0,11		<3	47	7	1,30	129
Øvstabø brook	30.07.2020		5,61	8,5	19	6	0,21	0,14	1,5	1,0				34	7		39
Øvstabø river	30.07.2020		5,62	8,2	24	7	0,23	0,13	1,3	1,0				37	5		63
Djupvatn brook	30.07.2020		5,67	11,8	23	8	0,26	0,23	2,2	1,4				40	8		81
Hunnevatn outlet	30.07.2020		5,54	8	20	6	0,19	0,12	1,3	0,9				36	6		21
Hunnemo	30.07.2020		5,62	5,8	17	6	0,08	0,10	0,8	0,7				34	6		52
Lake Hunnevatn 0m	30.07.2020	11,2	5,56	8,2	19	7	0,14	0,13	1,3	0,9	0,07		<3	35	10	0,83	32
Lake Hunnevatn 5m	30.07.2020	11	5,58	8,2	17	7	0,14	0,13	1,3	0,9	0,10		<3	35	9	0,83	44
Lake Hunnevatn 10m	30.07.2020	10,9	5,58	8,2	17	7	0,16	0,11	1,3	0,9	0,13		<3	32	7	0,75	60
Lake Hunnevatn 20m	30.07.2020	8,1	5,44	11,2	14	6	0,18	0,14	2,0	1,3	0,13		<3	30	13	0,81	48

Location	Date	Temp. (C)	pH	Conductivity (µS/cm)	Color (mg Pt/l)	ALKe (µeq/l)	K (mg/l)	Ca (mg/l)	Cl (mg/l)	Na (mg/l)	Mg (mg/l)	Diss-P (µg/l)	Tot-P (µg/l)	Al (µg/l)	LAl (µg/l)	SO_4 (mg/l)	NO_3 (µg/l)
Gilja	28.08.2020		6,21	17,9	21	24	0,17	0,47	2,9	2,1				30	5		253
Byrkjedal	28.08.2020		5,84	17,4	27	9	0,07	0,29	3,0	2,0	0,24		<3	35	6	1,40	113
VM byrkjedal	28.08.2020		6,29	15,6	18	21	0,18	0,42	2,3	1,8	0,23		<3	22	3	1,31	240
Øvstabø brook	28.08.2020		5,73	9	14	8	0,07	0,14	1,5	1,0				30	7		90
Øvstabø river	28.08.2020		5,87	11,2	19	11	0,09	0,25	1,6	1,2				24	5		92
Djupvatn brook	28.08.2020		5,85	11,3	22	10	0,08	0,21	2,1	1,4				32	5		87
Hunnevatn outlet	28.08.2020		5,66	8,4	22	9	0,11	0,15	1,4	0,9				36	10		-4
Hunnemo	28.08.2020		6,01	9,2	9	16	0,11	0,20	1,2	1,1				22	7		130
Lake Djupavatn 0m	28.08.2020	13,6	5,81	11,4	23	11	0,10	0,24	2,1	1,4	0,19		<3	31	4	0,90	56
Lake Djupavatn 5m	28.08.2020	13,4	5,76	12,2	24	11	0,19	0,23	2,1	1,4	0,17		<3	31	2	0,89	75
Lake Djupavatn 10m	28.08.2020	8,7	5,54	14,4	19	10	0,16	0,28	2,6	1,7	0,23		<3	32	6	0,87	50
Lake Djupavatn 20m	28.08.2020	5,3	5,43	16,4	20	10	0,20	0,32	2,9	1,8	0,25		<3	35	13	0,93	37
Gilja	18.09.2020		6,13	18,6	24	28	0,28	0,51	3,1	2,2				34	2		260
Byrkjedal	18.09.2020		5,78	16,7	28	14	0,15	0,30	3,2	2,0	0,24		<3	41	7	1,30	142
VM byrkjedal	18.09.2020		6,19	16,1	18	23	0,20	0,48	2,6	1,8	0,24		<3	27	5	1,43	291
Øvstabø brook	18.09.2020		5,68	9,8	15	10	0,18	0,18	1,7	1,1				29	8		75
Øvstabø river	18.09.2020		5,81	11,1	20	14	0,20	0,29	1,8	1,2				30	7		119
Djupvatn brook	18.09.2020		5,8	12,1	26	13	0,11	0,29	2,2	1,3				33	6		116
Hunnevatn outlet	18.09.2020		5,6	9,4	26	10	0,12	0,18	1,5	1,0				41	11		46
Hunnemo	18.09.2020		5,92	10,1	17	15	0,19	0,20	1,5	1,1				28	12		114
Lake Hunnevatn 0m	18.09.2020	10,1	5,59	9,5	25	10	0,12	0,16	1,5	1,0	0,08		<3	37	13	0,84	66
Lake Hunnevatn 5m	18.09.2020	9,9	5,6	9,9	28	11	0,12	0,18	1,6	1,0	0,10		<3	35	9	0,74	68
Lake Hunnevatn 10m	18.09.2020	9,8	5,59	9,4	28	10	0,08	0,16	1,5	1,0	0,10		<3	38	12	0,87	74
Lake Hunnevatn 20m	18.09.2020	9	5,53	9,1	25	10	0,08	0,18	1,6	1,0	0,11		<3	38	11	0,78	68

Location	Date	Temp. (C)	pH	Conductivity (µS/cm)	Color (mg Pt/l)	ALKe (µeq/l)	K (mg/l)	Ca (mg/l)	Cl (mg/l)	Na (mg/l)	Mg (mg/l)	Diss-P (µg/l)	Tot-P (µg/l)	Al (µg/l)	LAl (µg/l)	SO_4 (mg/l)	NO_3 (µg/l)
Gilja	16.10.2020		6,12	20,6	21	31	0,24	0,55	3,4	2,3				39	6		241
Byrkjedal	16.10.2020		5,85	17,2	26	20	0,12	0,36	3,2	2,1	0,22		<3	38	5	1,30	106
VM byrkjedal	16.10.2020		6,24	18,8	15	35	0,24	0,63	2,9	2,0	0,27		<3	25	6	1,46	268
Øvstabø brook	16.10.2020		5,71	10,5	12	14	0,19	0,23	2,0	1,2				29	5		66
Øvstabø river	16.10.2020		5,91	13,3	16	23	0,24	0,38	2,1	1,5				31	4		119
Djupvatn brook	16.10.2020		5,8	12,5	19	28	0,17	0,28	2,4	1,4				36	4		52
Hunnevatn outlet	16.10.2020		6,01	15,9	15	66	0,29	0,95	1,9	1,4				31	9		181
Hunnemo	16.10.2020		5,97	10,6	8	26	0,23	0,29	1,6	1,2				22	1		114
Lake Djupavatn 0m	16.10.2020	7,8	5,76	12,5	21	17	0,14	0,26	2,3	1,5	0,21		<3	37	10	0,90	55
Lake Djupavatn 5m	16.10.2020	7,3	5,76	12,7	23	18	0,17	0,26	2,4	1,5	0,20		<3	38	6	0,93	66
Lake Djupavatn 10m	16.10.2020	7,1	5,74	12,7	23	17	0,13	0,26	2,4	1,5	0,21		<3	38	9	0,85	59
Lake Djupavatn 20m	16.10.2020	7,1	5,75	12,7	23	16	0,13	0,26	2,3	1,5	0,18		<3	36	6	0,95	81
Gilja	01.12.2020		5,86	18,2	20	17	0,14	0,50	3,6	2,2				38	6		133
Byrkjedal	01.12.2020		5,46	16,3	27	14	0,16	0,33	3,2	1,9	0,22			44	7	1,43	46
VM byrkjedal	01.12.2020		5,82	15,4	17	18	0,22	0,42	2,9	1,7	0,24			32	9	1,21	133
Øvstabø brook	01.12.2020		5,47	11	16	7	0,07	0,16	2,2	1,2				34	12		19
Øvstabø river	01.12.2020		5,61	12	17	11	0,12	0,22	2,3	1,3				34	7		41
Djupvatn brook	01.12.2020		5,62	11,9	27	11	0,11	0,21	2,3	1,4				43	12		36
Hunnevatn outlet	01.12.2020		5,97	16,4	13	57	0,10	0,89	2,2	1,4				33	14		190
Hunnemo	01.12.2020		5,69	12,5	8	10	0,11	0,29	2,3	1,4	0,22			34	15	0,95	84